TUNABLE ERBIUM-DOPED FIBER RING LASER USING AN INTRA-CAVITY FILTER

A Thesis

by

HICHAM JOSEPH FADEL

Submitted to the Office of Graduate Studies of
Texas A&M University
in partial fulfillment of the requirements for the degree of

MASTER OF SCIENCE

August 2004

Major Subject: Electrical Engineering

TUNABLE ERBIUM-DOPED FIBER RING LASER USING AN INTRA-CAVITY FILTER

A Thesis

by

HICHAM JOSEPH FADEL

Submitted to Texas A&M University
in partial fulfillment of the requirements
for the degree of

MASTER OF SCIENCE

Approved as to style and content by:

Henry F. Taylor (Chair of Committee)	
Ohannes Eknoyan (Member)	Narasimha Reddy (Member)
John Criscione (Member)	Chanan Singh (Head of Department)

August 2004

Major Subject: Electrical Engineering

ABSTRACT

Tunable Erbium-Doped Fiber Ring Laser

Using an Intra-Cavity Filter. (August 2004)

Hicham Joseph Fadel, B.E., American University of Beirut

Chair of Advisory Committee: Dr. Henry F. Taylor

Linear tuning the frequency of an erbium-doped fiber ring laser using both a Fabry-Perot filter and an electro-optic tunable filter has been experimentally demonstrated. The rate of frequency change is determined by monitoring the fringes produced by laser light transmitted through a fiber Fabry-Perot interferometer.

The fiber ring laser has been tuned over a 50 nm spectral range when using the Fabry-Perot filter and a tuning rate of 16480 nm/s has been achieved. The spectral width of the laser is 0.049 nm and the nearest sidelobe to the main peak is more than 30 dB below the central lobe.

When the electro-optic tunable filter is used, a spectral range of 11 nm is reached. The spectral width is 2.33 nm and is in close agreement with the filter theoretical results. The sidelobe to main peak difference is around 13 dB.

To My Parents

ACKNOWLEDGEMENTS

I would like to express my deepest gratitude to Dr. Henry F. Taylor, the chairman of my advisory committee, for his continuous guidance and support during my research work. I would also like to thank Dr. Narasimha Reddy and Dr. John Criscione for serving as members of my graduate committee. I especially would like to thank Dr. Ohannes Eknoyan for his suggestions and advice throughout my research, and for also serving on my committee. My appreciation is also extended to Robert Atkins for his active cooperation. I also thank my colleagues Juan C. Juarez and Yang Ping for helping me and providing suggestions.

Special thanks go to my parents for their always-present love, support, and encouragement. And finally, my appreciation goes to my brothers and friends for always being there for me.

TABLE OF CONTENTS

Page

LIST OF FIGURES

FIGURE Page

FIGURE Page

LIST OF TABLES

TABLE Page

CHAPTER I

INTRODUCTION

During the past few years, the interest in wavelength division multiplexing in the 1.55 μm wavelength range has been growing, due to the excellent performance of optical fibers and the availability of compact optical amplifiers at this wavelength. Because of the increased bandwidth demand and the limited gain range of the erbium-doped optical amplifier, the channel spacing in WDM systems has been diminishing. This requires increasingly accurate wavelength control and flexibility to ensure reliable operation and world-wide interconnectivity.

Laser diodes are at the heart of every modern optical network. To exploit the fiber capacity beyond 40 Gbps, wavelength-division multiplexing (WDM) is widely employed. Multi-wavelength distributed feedback (DFB) laser arrays represent one solution, where each laser in the array operates at a particular wavelength. In their simplest form, these arrays have separate output for each array element. More sophisticated designs, like the one shown in Figure 1 integrate a combiner element that makes it possible to couple the light from multiple lasers to a single optical fiber without the use of complicated external coupling optics [1]. However, the wavelength tuning of the DFB lasers is very limited.

This thesis follows the style and format of *IEEE Journal of Lightwave Technology.*

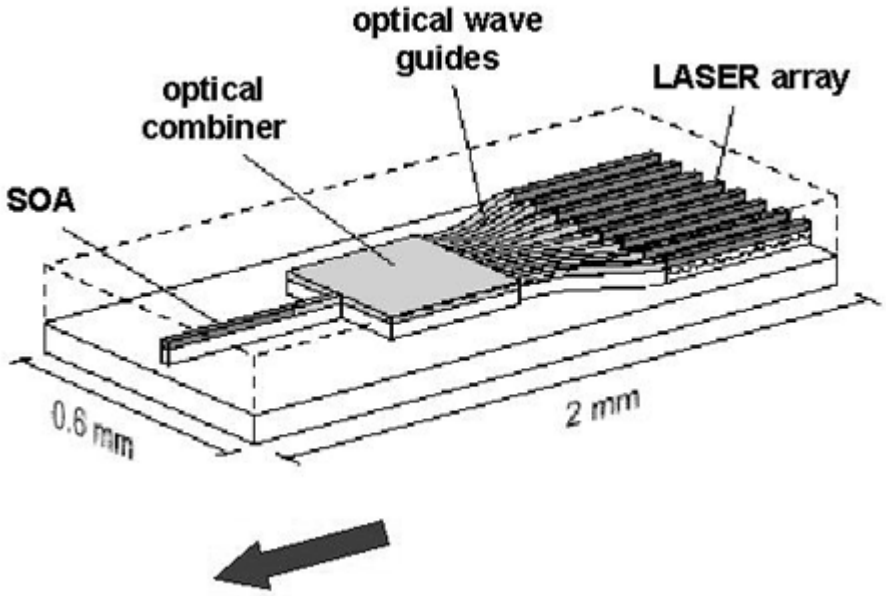

Figure 1. Multi-Wavelength DFB Laser Arrays; SOA = Semiconductor Optical Amplifier [2]

With demands for bandwidth still rising, lasers which are tunable over a broad (tens of nm) wavelength range are gaining more and more interest. Tunable laser technology, in conjunction with wavelength selective couplers and switches, is an enabling technology for rapidly reconfigurable fiber optic networks. Reconfigurability can lead to dramatic cost savings for metro and long haul networks, eliminating the need to install new equipment or rebuild the networks. The devices themselves are still semiconductor-based lasers that operate on similar principles to the basic non-tunable versions. Most designs incorporate some form of grating like those in a distributed feedback laser, but are much more complex in their implementation. These special

gratings can be altered in order to change which wavelengths they reflect in the laser cavity, usually by running electric current through them to alter their refractive index, a key property directly related to reflection properties. The tuning range of such devices can be as high as 40nm, which would cover any of 50 different wavelengths in a 0.8nm wavelength spaced system.

In this thesis research, a tunable erbium-doped fiber ring laser (EDFRL) using both an intra-cavity Fabry-Perot (FP) filter and an electro-optic (EO) filter as the tuning elements has been investigated. When the FP filter is used, tuning is achieved by varying the applied voltage which controls the FP cavity length; when the EO filter is used, tuning is also controlled with an applied voltage, but in this case the voltage alters the filter refractive index. The laser wavelength is monitored using an optical spectrum analyzer. When the laser is tuned rapidly, the frequency versus time characteristic is determined through the use of a fiber Fabry-Perot interferometer (FFPI) with a photodetector to convert the optical signal to an electrical signal.

A brief theoretical review is given in Chapter II. The system configuration and setup are described in Chapter III. Experimental results are discussed in Chapter IV. Finally, conclusions are summarized in Chapter V.

CHAPTER II

THEORETICAL BACKGROUND

A. Fiber Ring Lasers

A tunable EDFRL is shown in Figure 2.

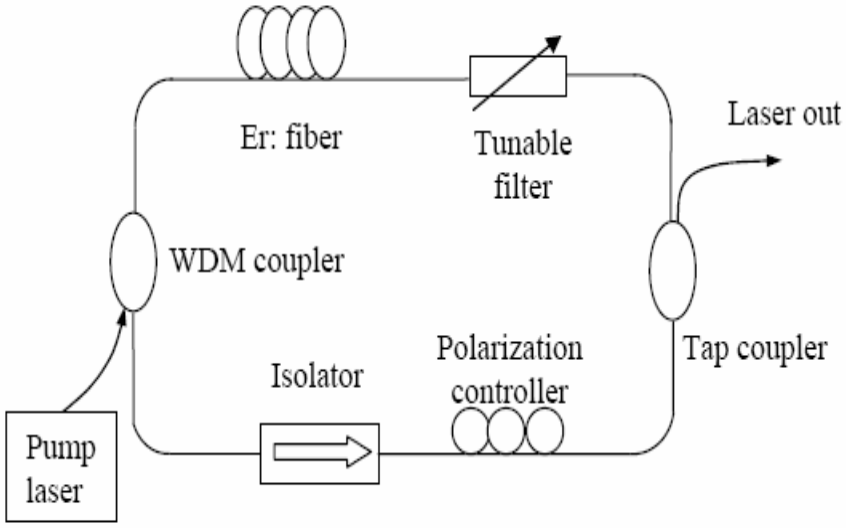

Figure 2. Schematic Illustration of a Tunable Erbium-Doped Fiber Ring Laser

Pumping the laser normally utilizes a laser diode emitting near wavelengths of 980 nm or 1480 nm, which correspond to the erbium-doped fiber spectral absorption

peaks. The pump light is coupled into the cavity by a wavelength division multiplex (WDM) coupler. The birefringence of the fiber is compensated with a polarization controller. A Faraday isolator ensures that the light travels only in one direction inside the laser cavity. The tunable bandpass filter is connected so that the laser wavelength can be tuned within the wide erbium-doped fiber gain spectrum span ranging from 1520 nm to 1570 nm. Slope efficiency of 10% ~ 15% is commonly achieved in this type of laser, which gives an output power in the order of mw. Multiple longitudinal mode operation is expected when the laser is operated in a continuous condition [3-4].

The tunable filter, the erbium-doped fiber, the WDM coupler and the Faraday isolator are key elements in the EDFRL design. A short review of each component follows.

1. Tunable Filters

Tunable filters provide flexibility in implementation of dynamic WDM systems and networks. Since in WDM systems each channel is related to a different wavelength, channel manipulation and particularly channel selection require some form of optical wavelength filtering. Important filter parameters include low insertion loss, high bandwidth, high sidelobe suppression, rapid tuning, small size, and low price. The various filter technologies are being designed in a way to best fit the above parameters in WDM applications. Generally, tunable optical filters can be divided into two main categories:

- Slow-speed tunable, with tuning times up to a few milliseconds, relevant for circuit-switched networks
- High-speed tunable, in the microsecond and nanosecond range, relevant for packet- and cell-switched networks

Different technologies are used to implement tunable optical filters. Candidate approaches include [5]:

- Filters based on the wavelength dependence of interferometric phenomena, such as Fabry-Perot and Mach-Zehnder filters
- Filters based on the wavelength dependence of coupling between optical fields induced by external perturbations, such as acousto-optic and electro-optic filters
- Filters based on semiconductor resonant structures

The filter technology pursued in this research corresponds to the first and second categories, the FP filter and the EO tunable filter, which will be discussed in Chapter III.

2. Erbium-Doped Fiber

An erbium-doped fiber consists of a short section of fiber that has a small amount of the rare earth element erbium added to it. The principle involved here is that erbium ions are able to exist in various electronic energy states: the ground (lowest energy state) and excited states. When an erbium ion is in an excited energy state, a photon of light can stimulate it to give up some of its energy to the light beam and return to a more stable lower energy state. This is called stimulated emission.

In such applications, a pump laser diode generates a high powered beam of light at a wavelength such that the erbium ions will absorb it and jump to an excited state. And as mentioned earlier, light emitted at 980nm or 1480nm can be used, because those wavelengths correspond to the erbium spectral absorption peaks.

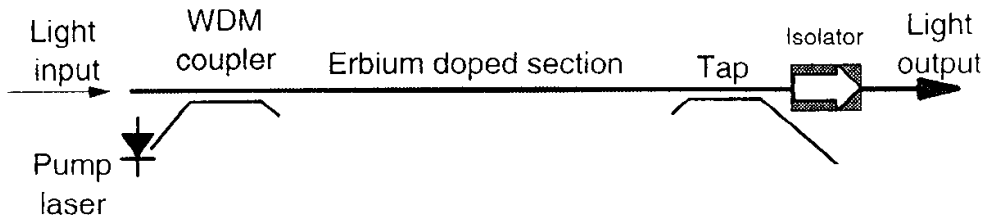

Figure 3. Erbium-Doped Fiber Amplifier [6]

The operation, depicted in Figure 3, goes as follows:

1. A relatively high-powered beam of pump light is mixed with the input signal in a single mode fiber using a wavelength selective coupler; the input signal and the pump light being at significantly different wavelengths.
2. The signal and pump light are guided into a section of fiber with erbium ions included in the core.
3. The pump light is absorbed by the erbium ions, exciting them to a higher energy state.
4. When the signal photons (at a longer wavelength than the pump light) pass through the erbium-doped fiber, some of the excited erbium atoms give up some of their energy to the signal and return to the lower energy state, by the process of stimulated emission.
5. The erbium ions give up their energy in the form of additional photons which are exactly in the same phase and direction as the signal being amplified. So the signal is amplified along its direction of travel only. Thus all of the additional signal power is guided in the same fiber mode as the incoming signal.
6. The isolator placed at the output prevents reflections returning from the attached fiber. This optical feedback would tend to destabilize the laser signal.

In this thesis research, the pump laser diode emits at 980nm. The application of the erbium-doped fiber as the gain medium in a laser will be discussed in Chapter IV.

3. WDM Couplers

Wavelength selective couplers are used to either combine or split light of different wavelengths, with minimal loss. Light of two different wavelengths on different input fibers can be merged onto the same output fiber (Fig. 4). In the reverse direction, light of two different wavelengths on the same fiber can be split so that one wavelength goes to one output fiber and the other wavelength is sent onto the other output fiber. The process can be performed with very little optical loss [6].

The coupling length over which power transfers from one waveguide to another is wavelength dependent. Thus, the shifting of power between the two parallel

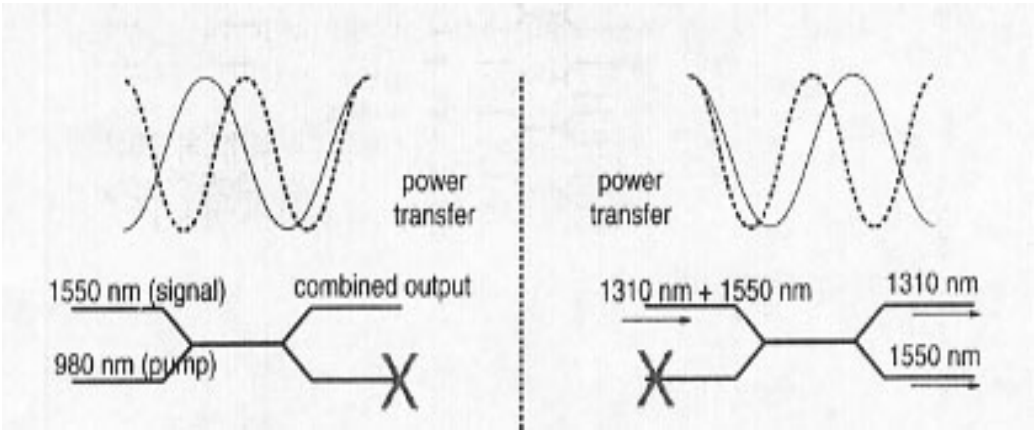

Figure 4. Power Transfer of Light in a Region Where Two Waveguides Are Merged [6]

waveguides will take place at different places along the coupler for different wavelengths. Figure 4 demonstrates the process: the graph of power transfer shows how power input on one of the fibers shifts back and forth between the two waveguides. The period of the shift is different for the two wavelengths. Thus, in the left hand section of the diagram there will be a place down the coupler where all of the light is only in one waveguide. By making the coupler exactly this length, the signals will combine and emerge from one output. On the right hand side of the diagram, the reverse process is shown where two wavelengths arrive on the same input fiber. At a particular point down the coupler, the wavelengths will be in different waveguides and by making the coupler have that exact length, the two input signals are separated. The process described here is performed with the same coupler, so it is bi-directional.

The WDM coupler used in this experiment combines light at 980nm from the pump laser diode with signal laser light at 1550nm.

4. Faraday Isolators

Because laser diodes are well known to be sensitive in particular to light energy reflected back from the rest of an optical setup, Faraday isolators are used to ensure a low level of return to the source.

The reflected light increases the noise in the transmitted beam, degrading system performance. Major oscillations in the signal come from reflections close to the transmitter. The measure of effectiveness in controlling reflections is the return loss. Expressed in decibels, it is defined as

$$L_R = -10 \times \log\left(P_R / P_I \right) \quad (1)$$

where P_I is the power incident on the component and P_R is the power reflected.

An optical isolator can be described as a one way transmission line. That is, it will allow propagation in only one direction along the fiber. Figure 5 shows a basic structure of an isolator. It consists of two linear polarizers and a 45 degrees Faraday rotator. For the two polarizers, the arrow is in the direction of the transmitted linear polarization component [7].

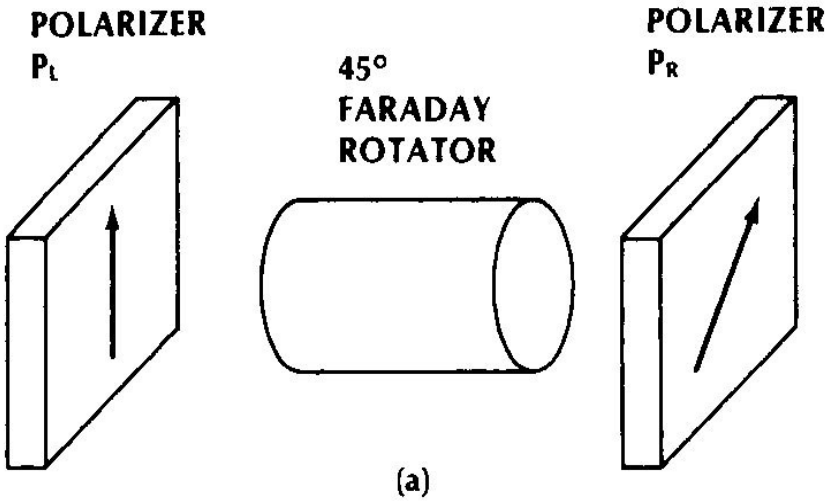

Figure 5. Basic Structure of a Faraday Isolator [7]

Figure 6 illustrates the operation: A beam of light incident from the left is vertically polarized by polarizer P_L, and in turn rotated by 45 degrees when passing

through the Faraday rotator. Thus, the beam emerging from the latter is linearly polarized at 45 degrees to the vertical, and is transmitted through polarizer P_R. No light can travel from right to left through the isolator; the only way transmission occurs is from left to right.

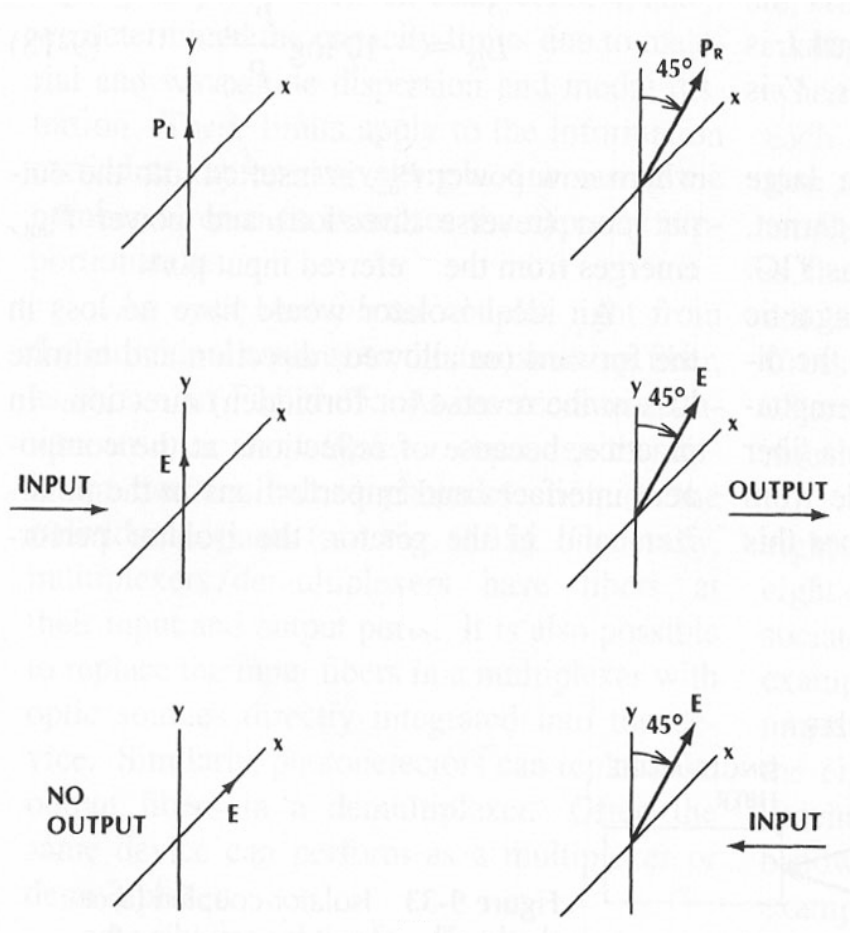

Figure 6. Graphical Operation of a Faraday Isolator [7]

Tunable lasers are a major enabling technology for the "all-optical network," and they do their part toward increasing network efficiency and flexibility, and simplifying

the process of service provisioning. In particular, the EDFRL of Figure 2 offers several desired features, such as:

- The potential for tuning over very wide wavelength ranges and easy wavelength tuning for testing wavelength division multiplexed optical technologies
- High output power for WDM fiber optic systems

B. Fiber Fabry-Perot Interferometer

The fiber Fabry-Perot interferometer consists of two internal dielectric mirrors separated by a length L of single mode optical fiber (Fig. 7).

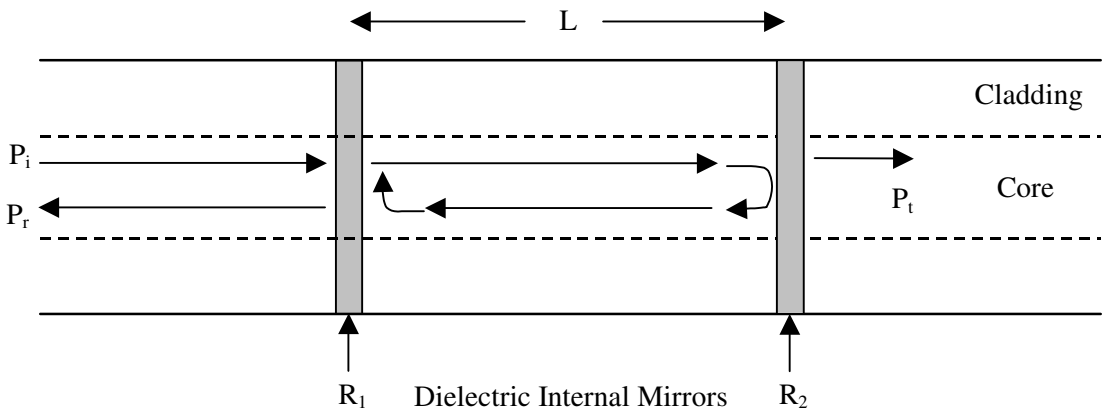

R_1 ,R_2 : reflectances
P_i : input power
P_r : reflected power
L : interferometer cavity length
P_t : transmitted power

Figure 7. Fiber Fabry-Perot Interferometer

The reflectance, R_{FP}, from the FFPI can be written as

$$R_{FP} = \frac{P_r}{P_i} = R_1 + R_2 + 2\sqrt{R_1 R_2}\cos\phi \tag{2}$$

with P_r the reflected optical power, P_i the incident optical power, ϕ the round-trip optical phase shift, and mirror reflectances R_1 and $R_2 << 1$. If the reflectances R_1 and R_2 are the same, with $R = R_1 = R_2$, R_{FP} can be expressed as

$$R_{FP} = \frac{P_r}{P_i} = 2R(1 + \cos\phi) \tag{3}$$

The round-trip phase shift of the light in the interferometer is given by

$$\phi = \frac{4\pi v n L}{c} = \frac{4\pi n L}{\lambda} \tag{4}$$

with L the cavity length of the interferometer, v the optical frequency of the laser light, n the refractive index of the fiber mode, c the free-space speed of light and λ the free space wavelength of the light source.

The change in ϕ caused by variations in length ΔL, frequency Δv and temperature ΔT can be expressed as

$$\phi = \phi_o + \Delta\phi_L + \Delta\phi_v + \Delta\phi_T \tag{5}$$

with

$$\Delta\phi_L = \frac{4\pi n}{\lambda}\Delta L \tag{6}$$

$$\Delta\phi_v = \frac{4\pi}{\lambda}\left(n + v\frac{dn}{dv}\right)\Delta v \tag{7}$$

$$\Delta\phi_T = \frac{4\pi}{\lambda}\left(L\frac{dv}{dT} + n\frac{dL}{dT}\right)\Delta T \tag{8}$$

where ϕ_o is the initial round trip phase shift.

In this research, the dependence of laser frequency on time will be determined from the variation of the optical power transmitted through the FFPI. The reflected optical power as determined by interference of the reflected waves from the two mirrors in the interferometer is converted into an electrical signal by a photodetector, and this signal is processed to obtain the value of the measurand of interest.

CHAPTER III

SYSTEM IMPLEMENTATION

A. Test System Configuration

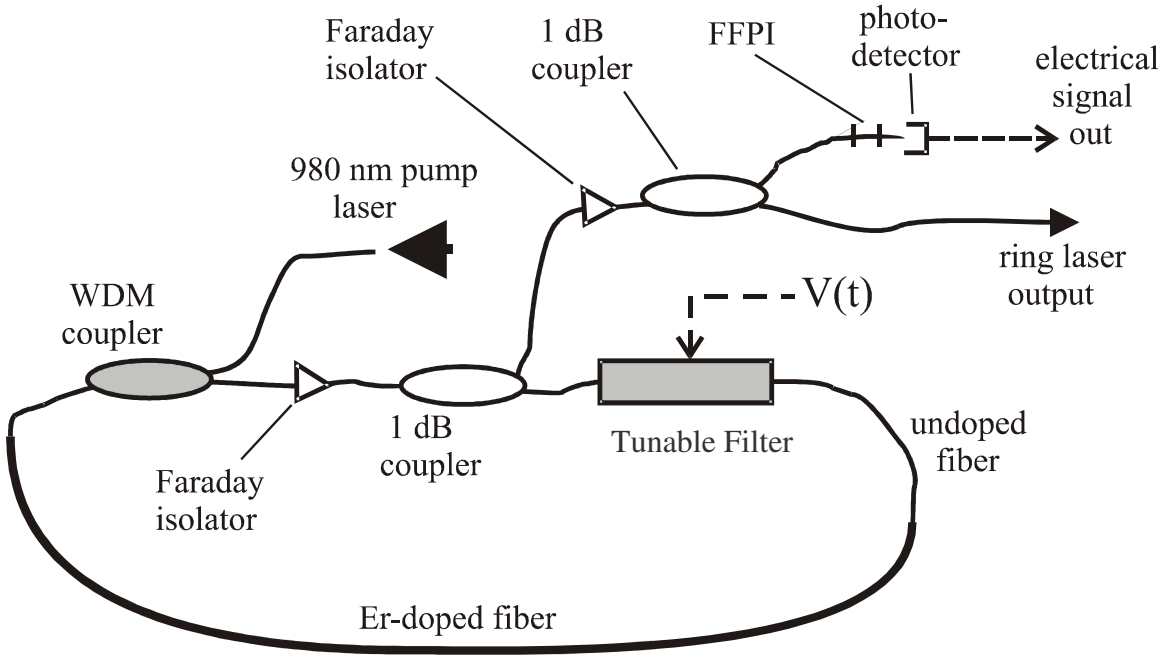

Figure 8. Tunable Ring Laser Test Setup

The ring laser shown in Figure 8 has been assembled in the laboratory, and its static and dynamic wavelength tuning characteristics have been studied. The semiconductor pump laser emits at 980 nm. The erbium-doped fiber section is 6 meters

long. The 1 dB couplers transmit approximately 20% of the light in the upper path and 80% in the lower path. The Faraday optical isolators, as described in Chapter II, determine the propagation direction of the laser field and the WDM coupler is used to couple the 980 nm pump light into the cavity while allowing the 1550 nm light to circulate. The integrated tunable filter is either a FP filter or an EO filter, and their corresponding modes of operation are described later in this chapter.

Optical losses of the components in the laser cavity are estimated to be:

- 1 dB couplers: 1 dB loss each
- WDM coupler: 1 dB loss
- Faraday isolators: 1 dB loss each
- Filter: 3.5 dB loss (FP filter) and 13 dB (EO filter)

Thus, the total intra-cavity loss is expected to be 6.5 dB in the FP filter case, 16 dB in the EO filter case and with the erbium-doped fiber section having a maximum gain of 30 dB, the excess gain of the laser cavity is projected to be around 23.5 dB and 14 dB respectively.

The pump laser driving the whole circuit is configured as shown in Figure 9, the driving unit having a supply current of a maximum of 200 mA.

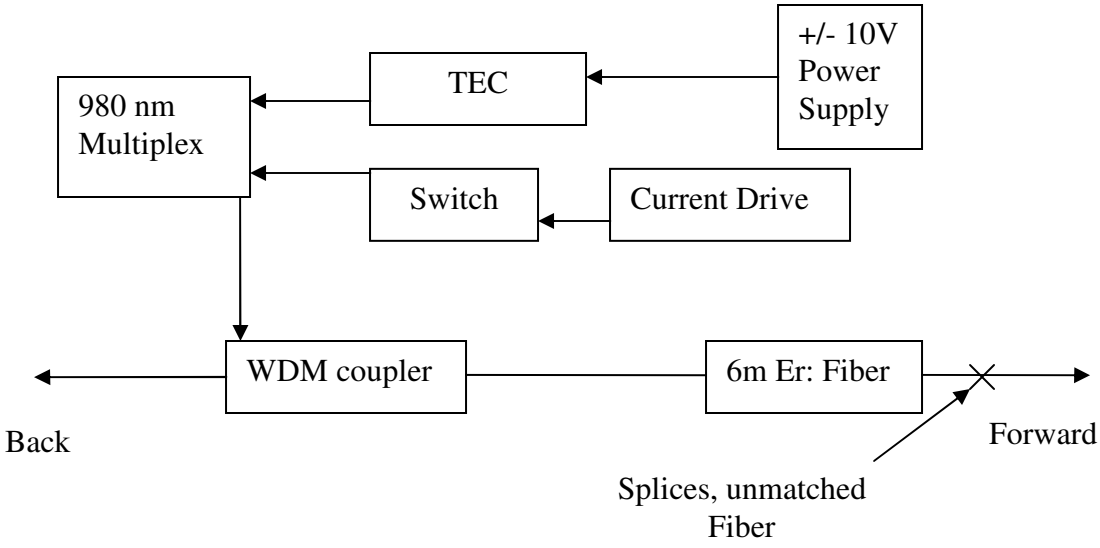

Figure 9. Pump Laser Internal Connections

B. The Fabry-Perot Tunable Filter

Fabry-Perot filters and interferometers have provided the highest known optical wavelength resolution for 100 years, and are still considered seminal instruments in many branches of science including astronomy, atomic physics, chemistry, lasers, metrology, optics, plasma physics and spectroscopy. The original optical configurations were constructed of bulk lenses, mirrors and beam optics along with geared positioning stages. However, in spite of their superior optical resolution, conventional bulk optic, Fabry-Perot devices have two fundamental problems:

- There is no method of guiding the light between the mirrors, which results in extreme sensitivity to alignment, temperature and vibration. With each bounce of the beam, some light walks-off and is lost.
- Mechanisms for moving the mirrors the extremely small atomic distances required to accurately tune or continuously scan the Fabry-Perot device while maintaining alignment are expensive.

The new Fabry-Perot technology (Fig. 10) consists of adding a single segment of optical fiber within the original etalon (optical cavity between two reflective surfaces). The high optical resolution advantage of the bulk optic device is preserved, but with three critical distinctions:

- The optical fiber inside the etalon guides the light with each bounce between the mirrors.
- The filter has natural fiber connection compatibility unlike lenses or integrated waveguides, which encounter fundamental connection difficulties.
- The filter is equipped with a high resolution mechanical positioning device, a piezoelectric transducer (PZT), to position the mirrors inside the etalon.

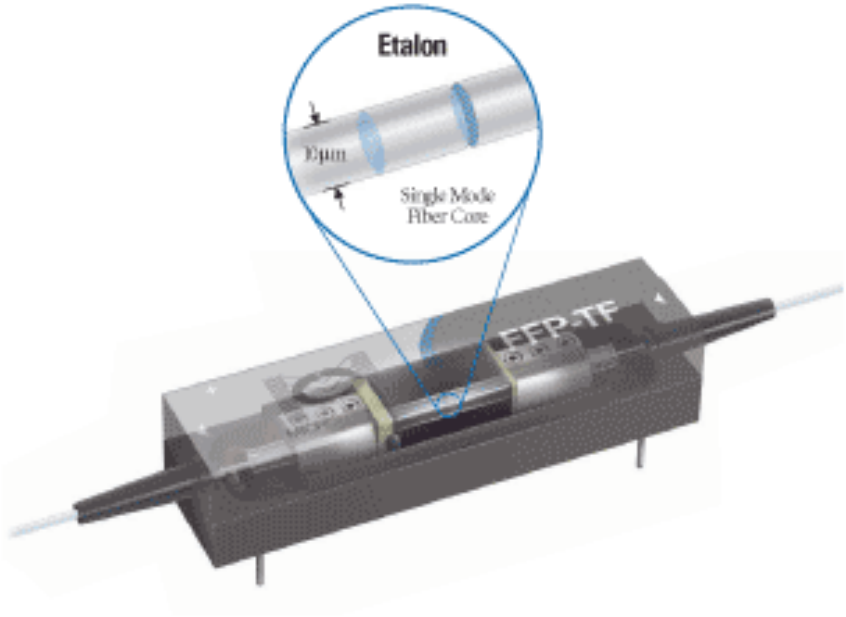

Figure 10. The Fabry-Perot Tunable Filter [8]

The commercial tunable filter used in this experiment is a specialized filter based on Fabry-Perot etalon technology, and is from Micron Optics. The filter passes frequencies that are equal to Nc / 2L, with N an integer, L the cavity length, and c the free space speed of light. The length is changed by applying voltage to the PZT, thus allowing tuning over a wide spectral range. The insertion loss is around 3.5 dB. The filter specifications are given in the Appendix.

C. The Electro-Optic Tunable Filter

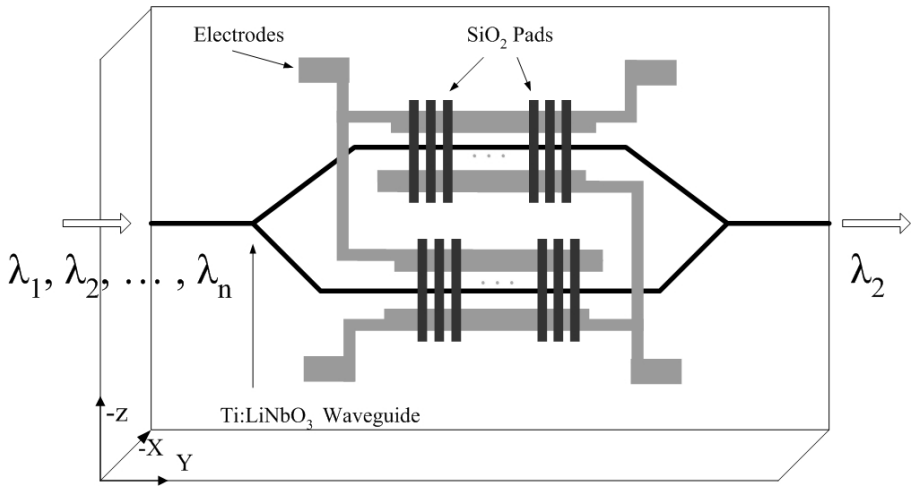

Figure 11. Electro-Optic Filter Configuration

The intra-cavity filter, developed previously at Texas A&M [9-10], is shown in Figure 3. The waveguides are single mode for both TE and TM polarizations. The Y-branches are symmetric 3-dB optical power splitters, and the optical path length difference for the waveguide arms between the two branching points is a half-wavelength. Phase-matched polarization coupling between orthogonal modes in the waveguide arms is achieved through a refractive index grating produced from a shear (S_6) static strain component that is induced by a spatially periodic SiO_2 surface film. The strain results from the thermal expansion mismatch between the substrate and film when the SiO_2 film is deposited at an elevated temperature and patterned at room

temperature. The spatial period of the strain-inducing pads Λ is the same along both arms of the waveguide and satisfies the phase-match condition:

$$\Lambda = \lambda_o / \Delta n \tag{9}$$

where λ_o is the free-space wavelength and Δn is the birefringence in the waveguide. However, the positions of the polarization coupling regions in the two waveguide arms are displaced relative to each by half of the spatial period, $\Lambda / 2$. Tuning of the phase-matched wavelength is accomplished by altering the waveguide birefringence electro-optically through the application of a voltage across the electrodes.

To achieve the lowest possible loss in the laser cavity, high-precision translation stages are used for aligning the input and output fibers with the filter. Three such stages, allowing motion along three space axis, are fixed on the optical table: the first one is for holding the filter; the second one is for aligning the input fiber; and the last one adjusts the position of the output fiber. Both input and output fibers are cleaved to produce a flat end. The cleaved fibers are cleaned using methanol and aligned perpendicularly to the filter axis in order to avoid scattering of light between the waveguide and the fibers.

The voltage on the electrodes is varied using a triangular or sawtooth waveform from a function generator. The dependence of laser frequency on time is determined from the variation of the optical power transmitted through the FFPI (Fig. 7). The photodetector current I is a sinusoidal function of optical frequency, given by

$$I = I_0 (C_1 + C_2 \cos\phi) \tag{10}$$

with I_0, C_1, and C_2 constants and ϕ, the round trip phase shift described in equation 4.

Thus, for example, if the laser frequency varies linearly with time ("linear chirp"), the photocurrent will vary sinusoidally with time at a frequency proportional to the chirp rate [4]. Discontinuous changes in the photocurrent vs. time data result from sudden alterations in the laser frequency, indicative of mode hops. The dynamic tuning characteristics of the laser have been investigated in this manner for different linear chirp rates.

CHAPTER IV

TEST RESULTS

A. Laser Characterization

In this chapter, experimental data on the erbium-doped fiber ring laser in different testing setups are given.

An optical spectrum analyzer (OSA) is used to measure the center wavelength at which the laser is emitting. In addition to the center wavelength, an upper limit to the spectral width of the emission line is also determined.

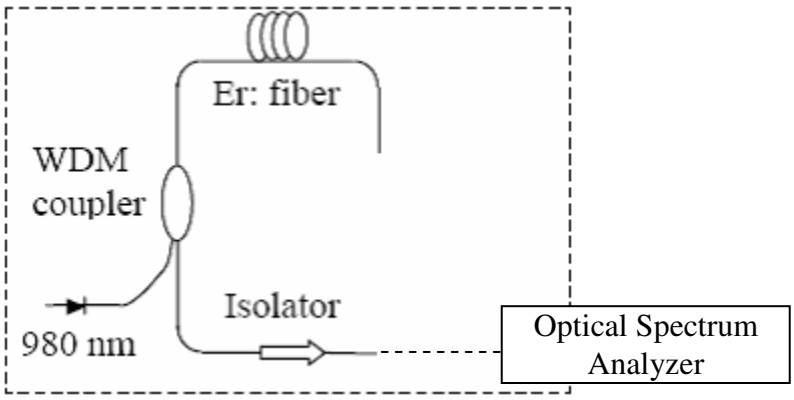

Figure 12. Erbium-Doped Fiber Laser with a Broken Ring

A series of experiments have been conducted to study the behavior of the erbium-doped fiber laser, which is pumped by a laser diode emitting at 980 nm, with a

pumping power of 35 mW. First of all, the ring has been broken, as shown in Figure 12, and one of the ends connected to the OSA. With no filter inside the cavity, only the erbium-doped fiber emission profile is observed, as shown in Figure 13. The center wavelength of the emitted light is 1531.58 nm and the spectral width is 4.44 nm.

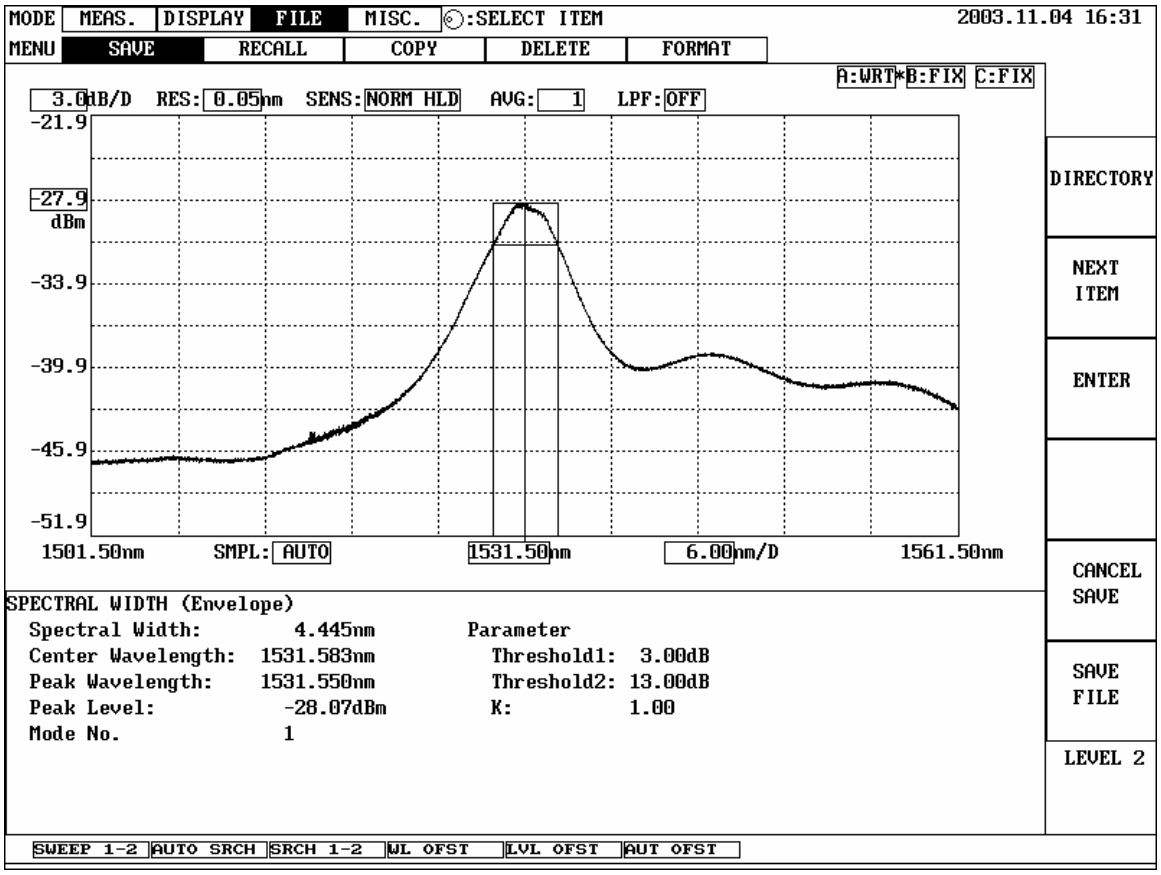

Figure 13. Erbium-Doped Fiber Emission Profile

Next, a fiber coupler is spliced to the isolator output, and one output port of the coupler is spliced to the erbium-doped fiber to form the ring cavity. The second coupler output is input to the OSA, as shown in Figure 14.

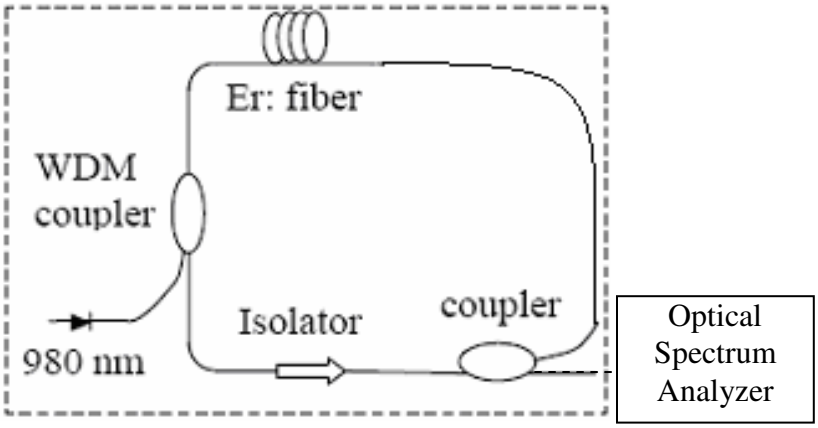

Figure 14. Erbium-Doped Fiber Laser with a Connected Ring Cavity

The optical spectrum analyzer does not detect any light signal near the pump laser wavelength of 980 nm. Evidently, the isolator and the tap coupler remove any unabsorbed pump light passing through the erbium-doped fiber.

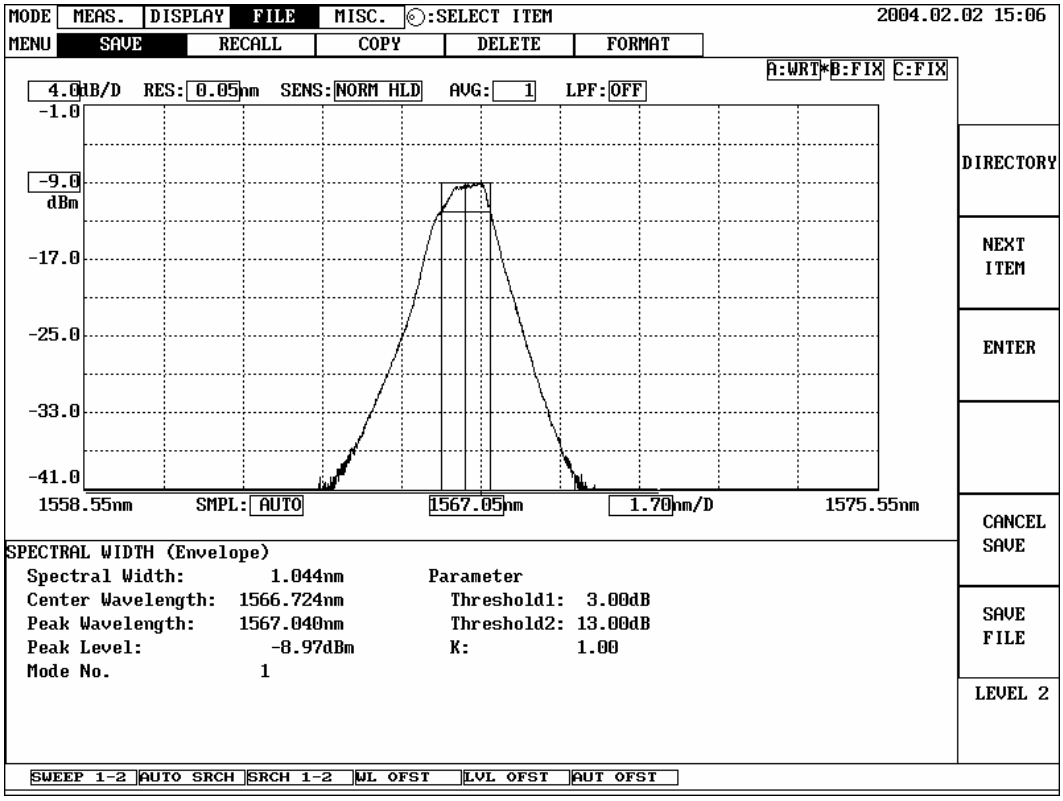

Figure 15. Single Wavelength Spectral Profile at 1566.72 nm

The only light signal detected by this setup is a sharp spectral line at 1566.72 nm, as shown in Figure 15. In addition to the center wavelength, the spectral width of the laser line is determined by the OSA to be 1.044 nm. The spectral width is here defined as the full width at half maximum power; i.e. where the laser power drops by 3 dB.

With the ring cavity formed, the lasing spectrum shown in Figure 15 is different from the amplified spontaneous emission spectrum in Figure 13; those differences are shown in Table 1.

Table 1 Ring Cavity Broken vs Ring Cavity Connected

	Center Wavelength	**Spectral Width**	**Peak output power**	**side lobes to main peak**
Ring cavity broken	1531.58 nm	4.445 nm	-28.07 dBm	10 dB
Ring cavity connected	1566.72 nm	1.044 nm	-8.97 dBm	30 dB

The peak output power is much bigger in the case of the connected cavity (lasing) because the light is constantly going through the erbium-doped fiber and thus being amplified. The spectral width of the connected cavity lasing profile is 3.4 nm narrower than the broken cavity (amplified spontaneous emission) profile. The side lobe to main peak difference is 10 dB in the spontaneous emission case and 30 dB in the lasing case.

B. Tunable Laser Characteristics (FP Filter)

The next test setup is very similar to the previous one, except that the ring cavity now includes the Fabry-Perot tunable filter presented in Chapter III. As Figure 16 shows, another isolator is added outside the cavity to ensure that no light will get reflected back to the laser, and the second coupler is used to split the light into two outputs: the first output goes to an optical power meter to relate the pump power to the laser power or to

the OSA to monitor the center wavelength and the spectral width, while the second output goes through a FFPI and then to a photodetector to investigate the dynamic tuning characteristics of the laser.

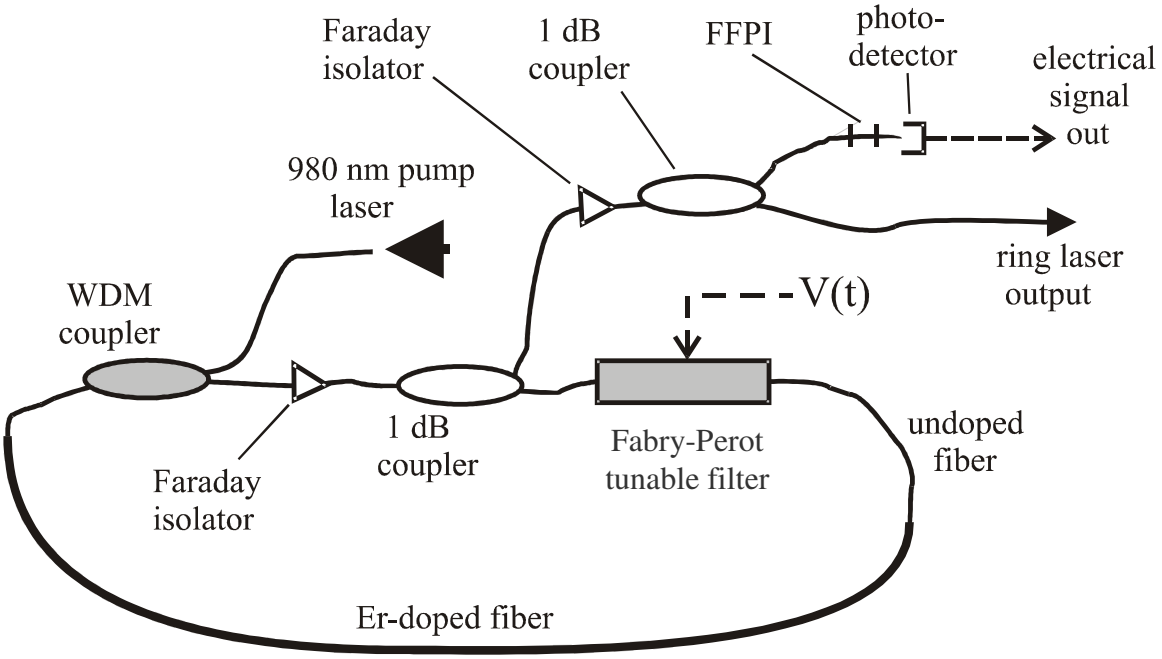

Figure 16. Tunable Ring Laser with a Fabry-Perot Filter

When the "ring laser output" end of Figure 16 is connected to an optical power meter, the laser power as a function of pump power can be recorded. Table 2 shows the relative values of the pump power and output power with the respect to the values of the current driving the EDFL. The laser power as a function of pump power is plotted and shown in Figure 17. The laser threshold pump power and slope efficiency are determined to be 11 mw and 11% respectively.

Table 2 Laser Power as a Function of Pump Power and Driving Current

Driving Current (mA)	Pump Power (mW)	Laser Output Power (mW)
20	0	0
31	11	9.00E-09
60	15	0.4
80	35	1.72
100	47	2.8
120	55	3.6
140	70	5.1
160	82	6.4
180	95	8.2
200	110	10.1

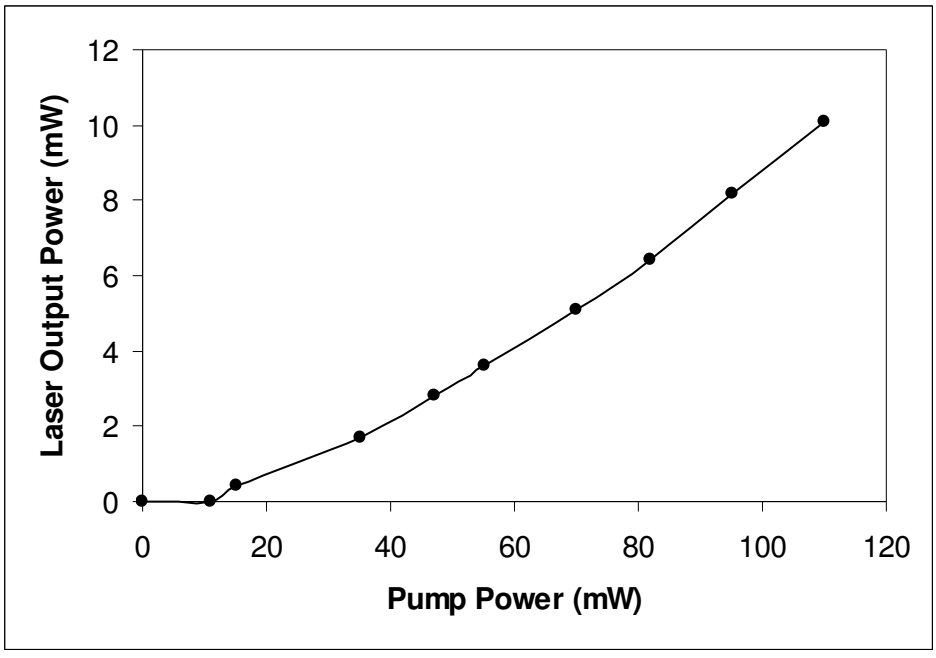

Figure 17. Laser Power vs Pump Power

Now the same end is disconnected from the optical power meter and replaced by the OSA. The Fabry-Perot tunable filter is connected to a DC power supply and the voltage is varied manually from 0 V to 7 V. Tests have been carried out at different voltages, and data has been collected at 0.5 V, 1 V, 2V, 3V, 5 V and 7V. The results are shown respectively in Figures 18 through 23. At 0 V, the lasing wavelength turned out to be 1539.3 nm, and then as the voltage increased, the wavelength reached 1589.35 nm. After 7 V, the Fabry-Perot tunable filter shifts to another transmittance peak and the lasing wavelength goes back to the beginning of the spectrum. The cycle is repeated continuously as we increase the DC voltage until we reach the maximum tuning voltage the filter can handle, which is 70 V.

The results clearly show a tuning range of about 50 nm. The spectral width is 0.049 nm and is almost constant over the entire spectrum. The peak power of every lasing profile, as observed in Figures 18 through 23, is almost fixed and the average value is measured to be around -1.4 dBm.

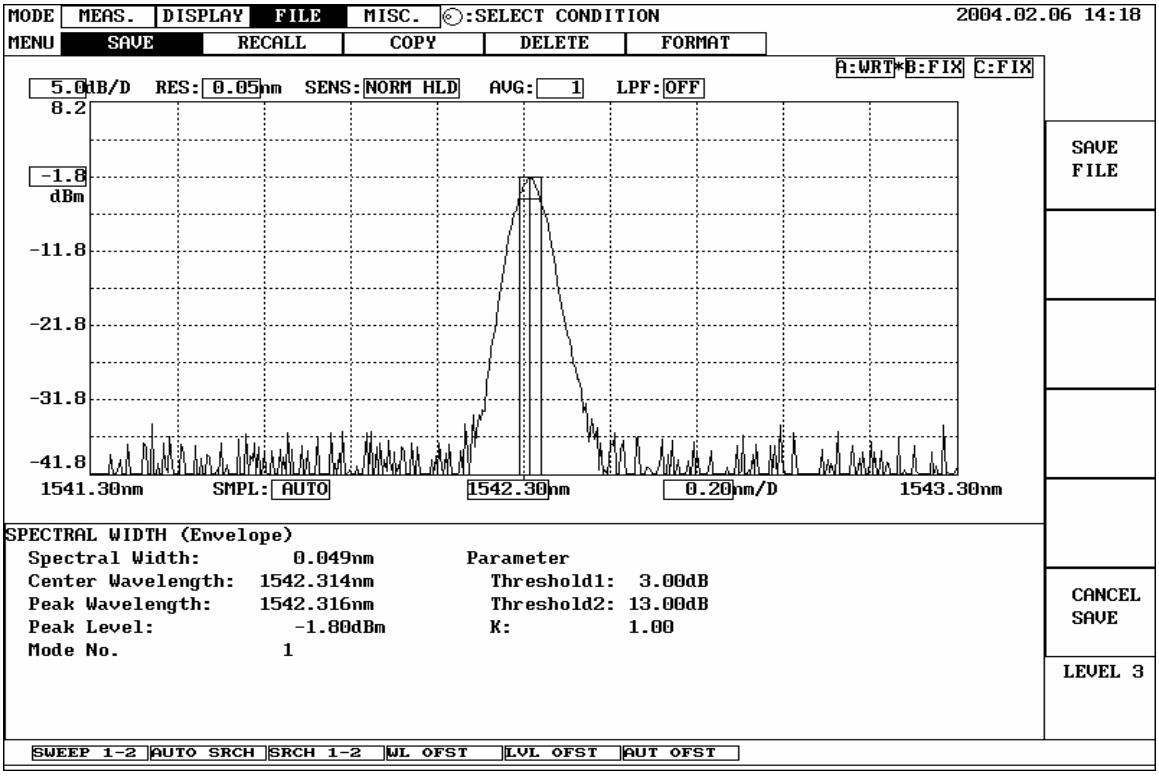

Figure 18. Laser Spectral Profile at DC Voltage = 0.5 V

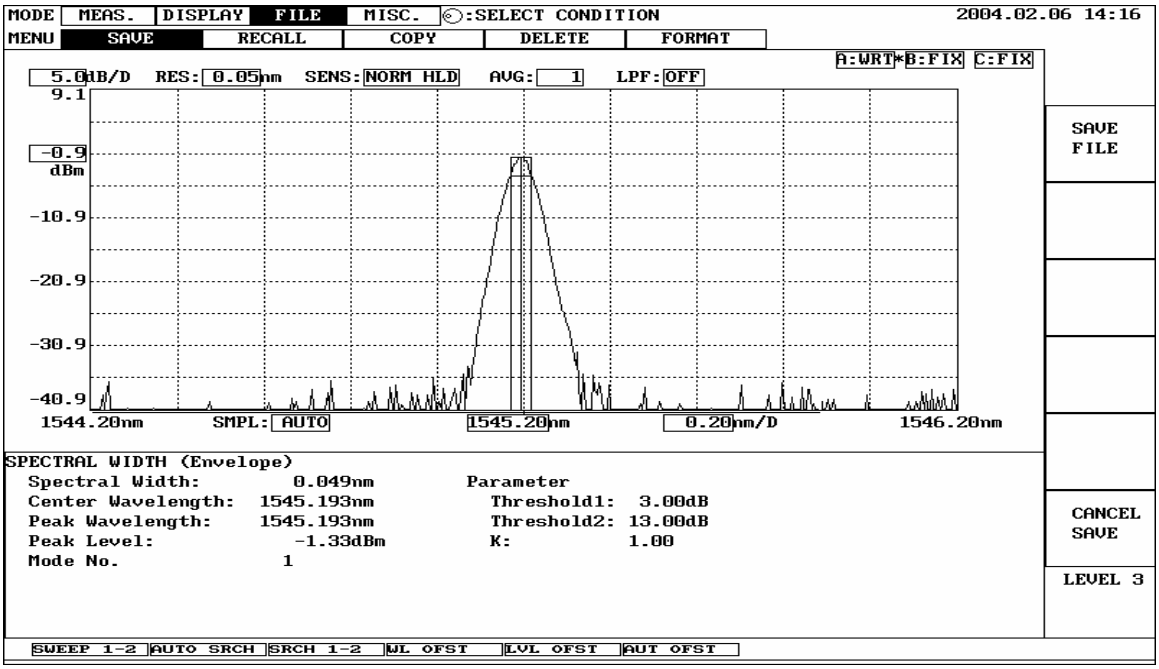

Figure 19. Laser Spectral Profile at DC Voltage = 1 V

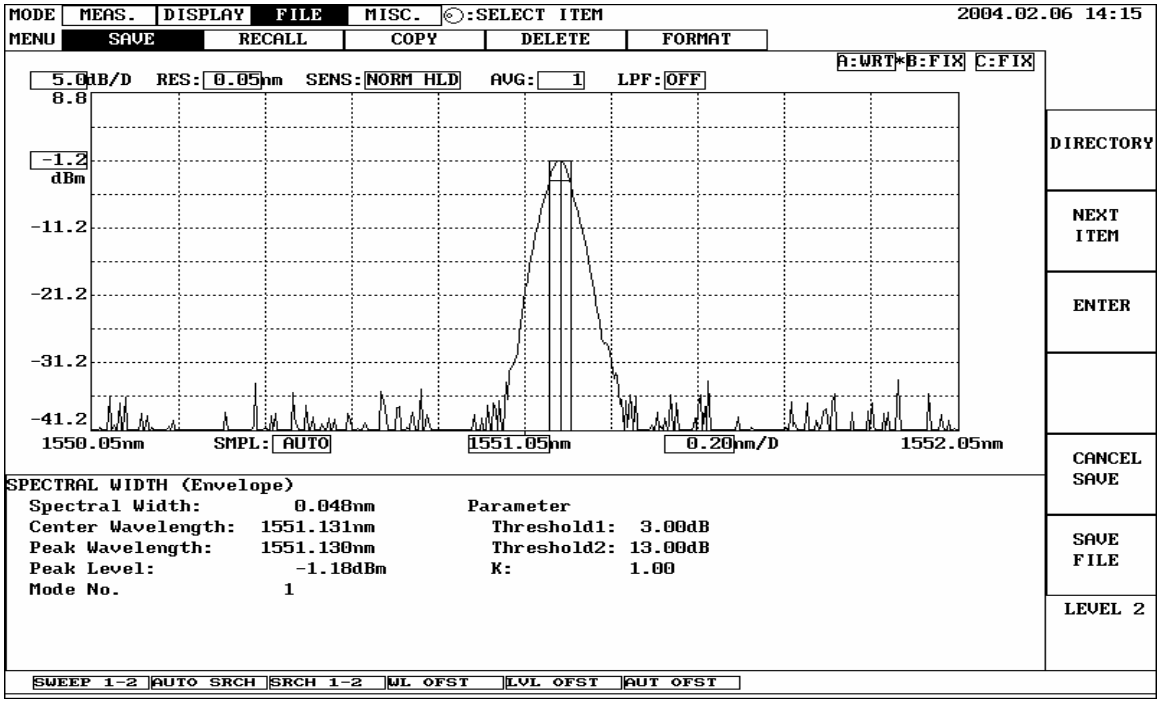

Figure 20. Laser Spectral Profile at DC Voltage = 2 V

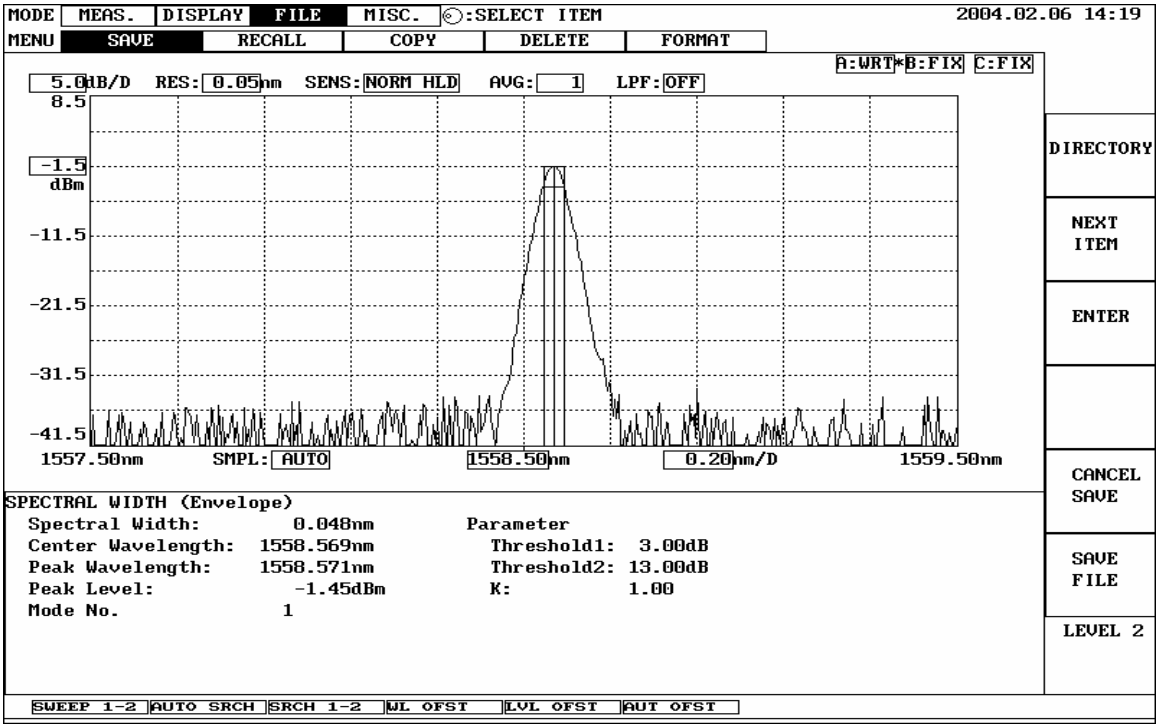

Figure 21. Laser Spectral Profile at DC Voltage = 3 V

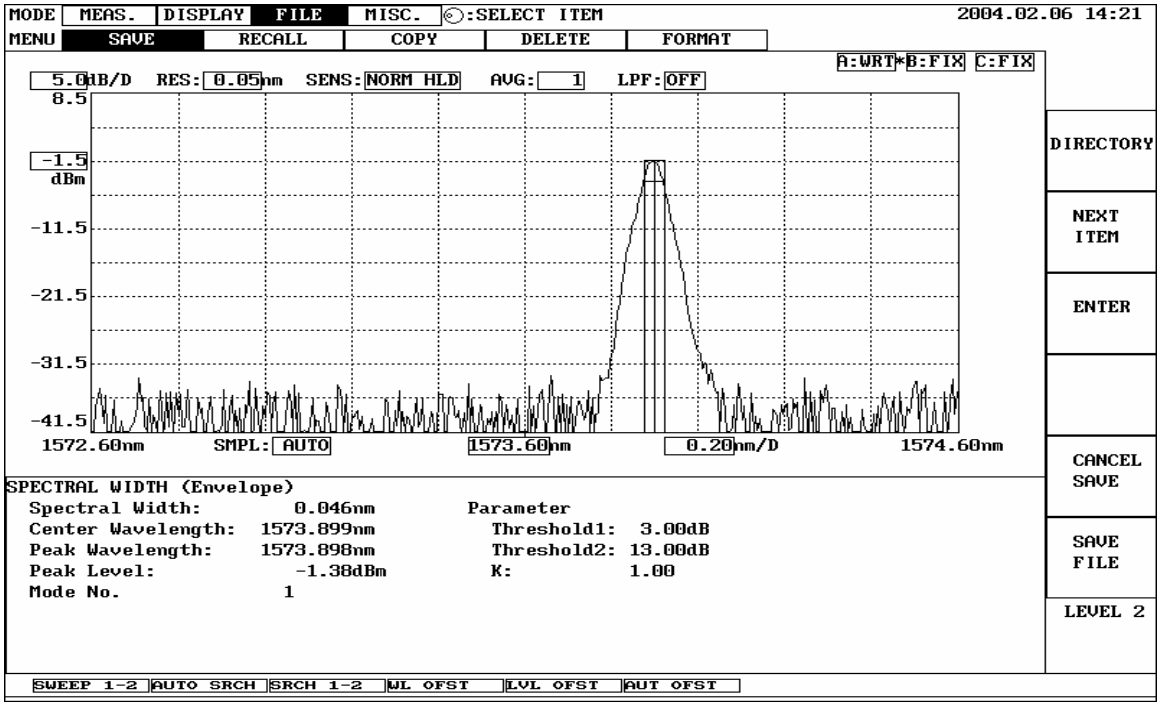

Figure 22. Laser Spectral Profile at DC Voltage = 5 V

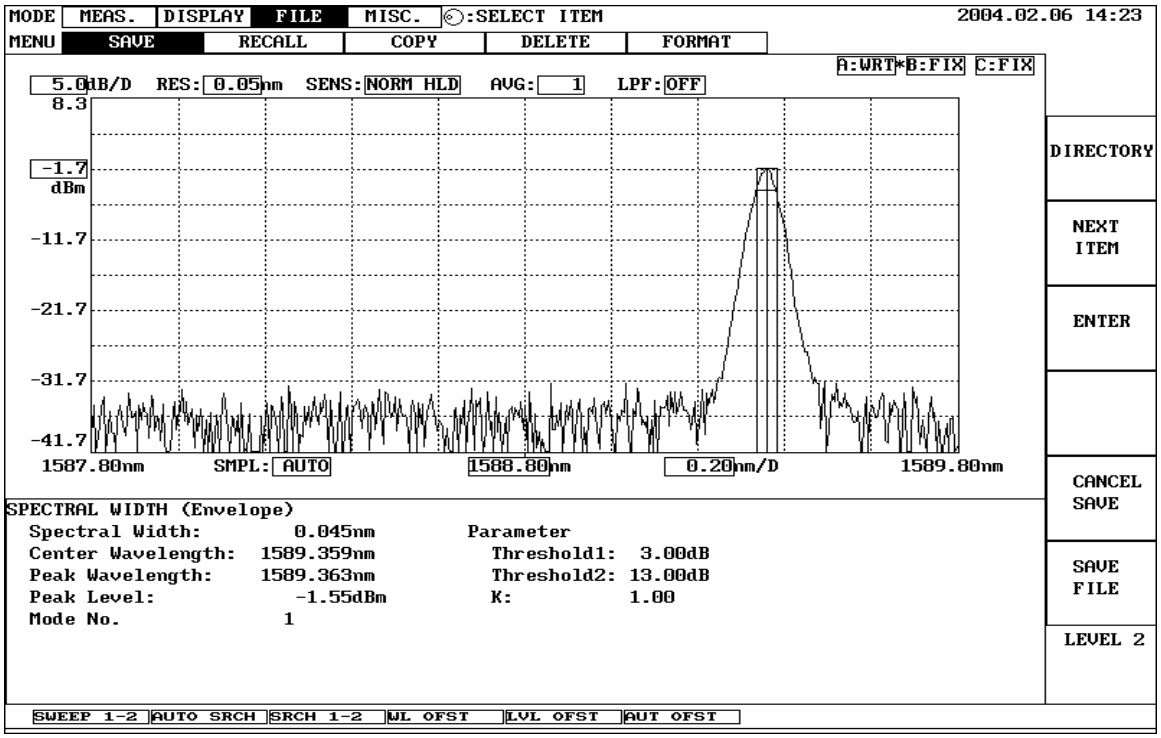

Figure 23. Laser Spectral Profile at DC Voltage = 7 V

C. Dynamic Tuning Characteristics

To investigate the dynamic tuning characteristics of the laser, the DC power supply connected to the filter is replaced by a function generator which produces a sawtooth waveform which varies from 0 V to 6 V. The frequency of the sawtooth waveform is varied from 0.2 Hz to 200 Hz.

The output connected to the OSA detected three lasing wavelengths as we scanned the spectrum, and the results are shown in Figure 24.

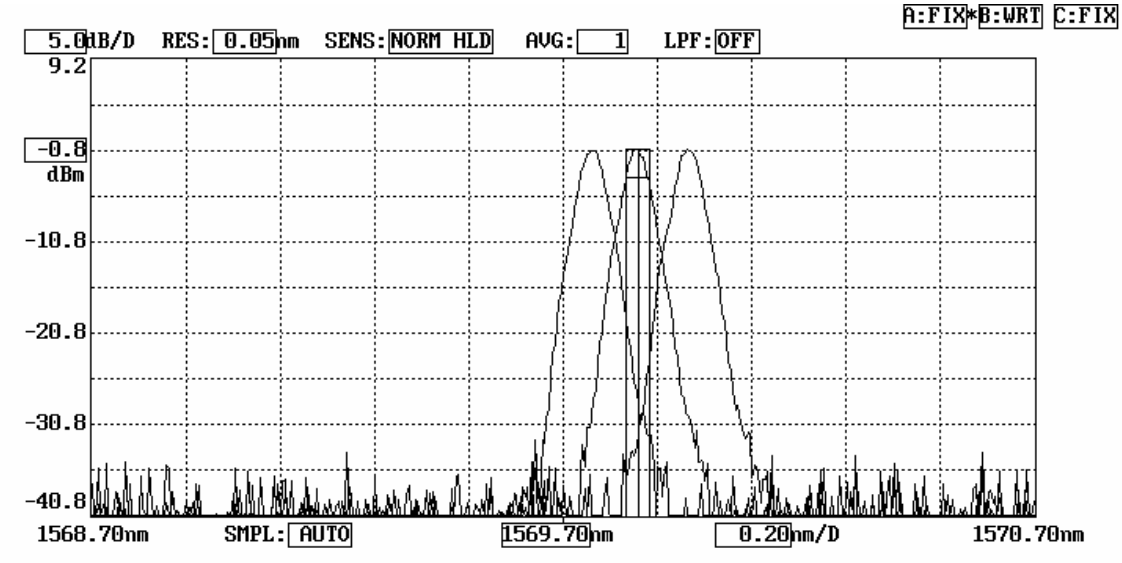

Figure 24. Scanning of Laser Spectrum (Span =2 nm)

The OSA clearly shows that the signals detected have the same characteristics except for the center wavelength. A “snapshot” of the spectrum was recorded at three different points in the spectral scan.

To demonstrate the tuning linearity of the laser, the dependence of the lasing wavelength on the tuning voltage is given in Figure 25, which shows that the wavelength is close to a linear function of voltage.

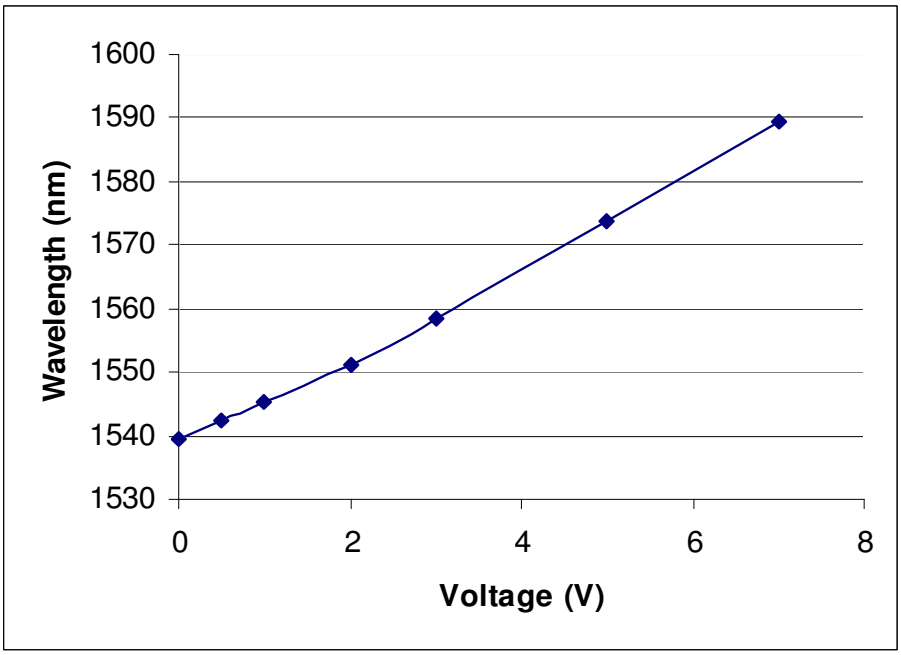

Figure 25. Wavelength vs Tuning Voltage (FP Filter)

To further illustrate this linear dependence, the "electrical signal out" end of Figure 16 is now connected to a Labview program to monitor the transmittance of the fiber Fabry-Perot interferometer. The dependence of laser frequency on time is determined from the variation of the optical power transmitted through the FFPI (Fig. 7) as the laser is tuned. The photodetector current I is a sinusoidal function of optical frequency, as described by equation 10.

Figures 26 through 29 illustrate how the transmittance of the FFPI varies with time when the sawtooth waveform frequency is varied from 0.2 Hz to 200 Hz.

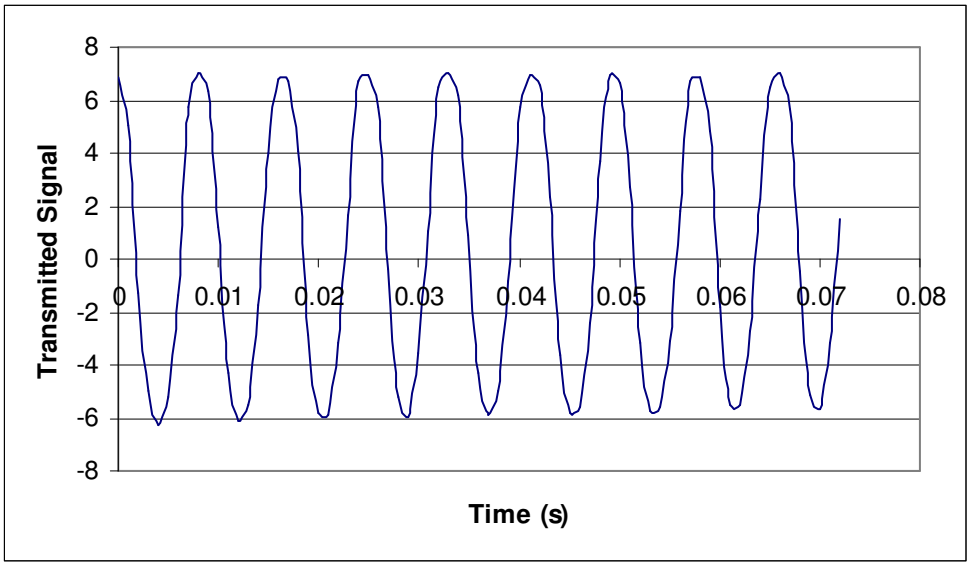

Figure 26. Transmittance of FFPI with a Sawtooth Frequency of 0.2 Hz

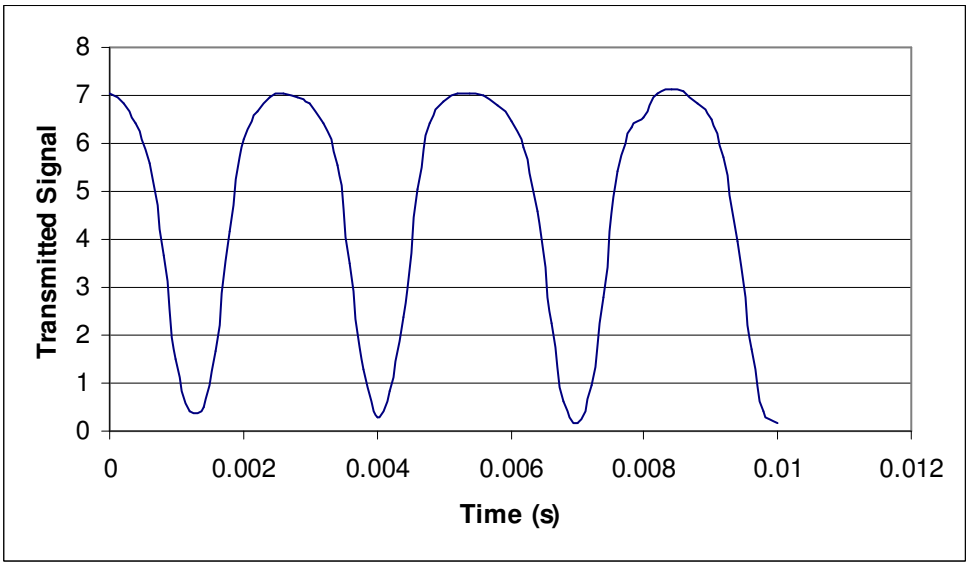

Figure 27. Transmittance of FFPI with a Sawtooth Frequency of 0.5 Hz

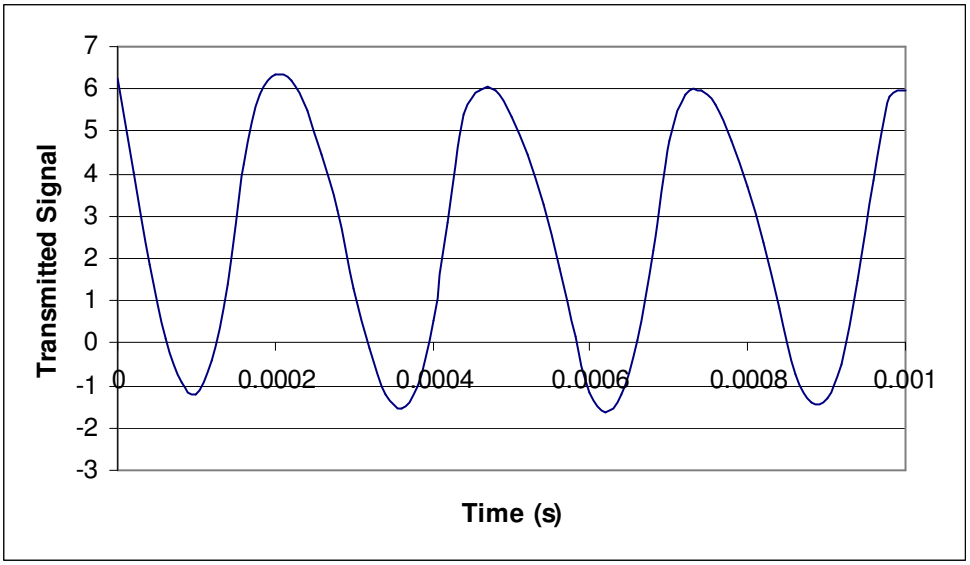

Figure 28. Transmittance of FFPI with a Sawtooth Frequency of 5 Hz

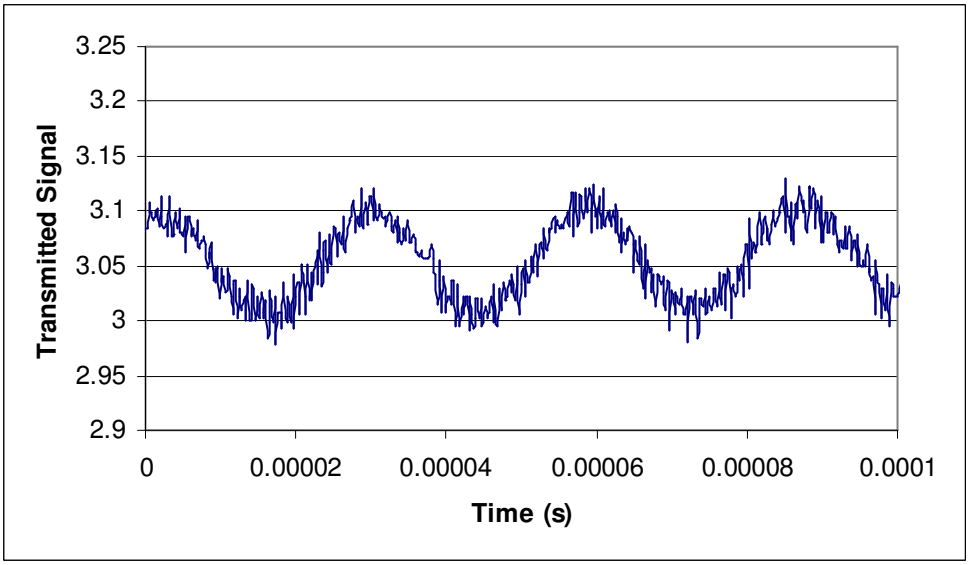

Figure 29. Transmittance of FFPI with a Sawtooth Frequency of 50 Hz

To further interpret these results, it follows from equation 4 that the frequency change for every 2π phase shift in the interferometer output (one fringe) is (c/2nL). With c = 3.10^8 m/s, n = 1.46 and L = 10mm, the frequency change per fringe is calculated to be 10.3 GHz.

The fringes in Figure 26 vary with a temporal period of 0.009 seconds. Therefore, the tuning speed at 0.2 Hz is (10.3 GHz / 0.009 s) = 1144.5 GHz/s, corresponding to approximately 10 nm/second.

If we do the same calculations for different sawtooth frequencies, we conclude that the tuning speed laser at 0.5 Hz, 5 Hz, 50 Hz and 200 Hz are 29.45 nm/s, 294.6 nm/s, 2749.5 nm/s and 16480 nm/s respectively.

Figures 26 through 29 can provide more valuable information as to the tuning linearity of the laser. By plotting the number of intersections of the sinusoidal function and the x axis with respect to time, we obtain another linear plot which is a function of the FFPI phase Φ. This is illustrated in Figures 30 through 33, corresponding respectively to Figures 26 through 29.

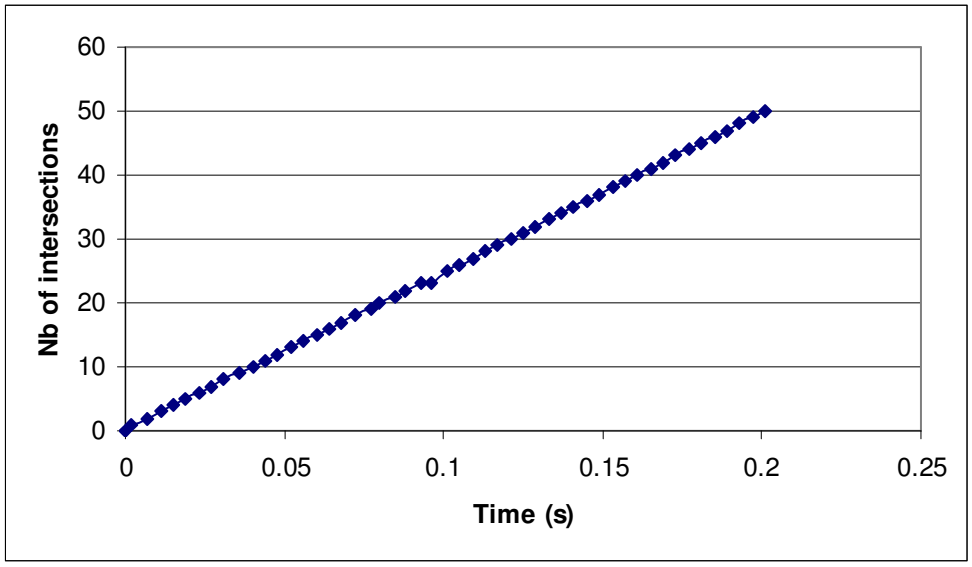

Figure 30. Number of Intersections of Figure 26 and X Axis (Half-Fringes) as a Function of Time as the Laser Is Tuned, for a Sawtooth Frequency of 0.2 Hz, Corresponding to a Tuning Rate of 10 nm/s

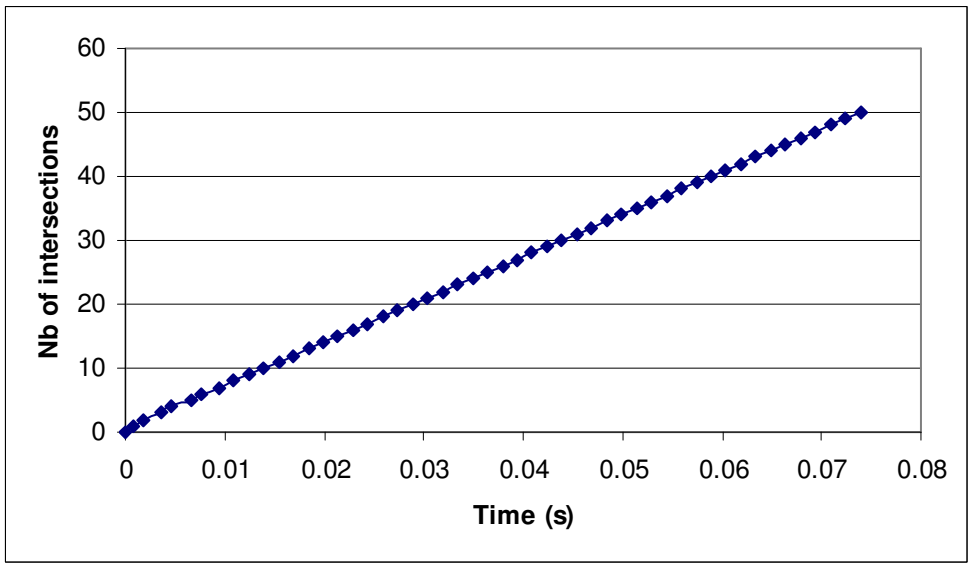

Figure 31. Number of Intersections of Figure 27 and X Axis (Half-Fringes) as a Function of Time as the Laser Is Tuned, for a Sawtooth Frequency of 0.5 Hz, Corresponding to a Tuning Rate of 29.45 nm/s

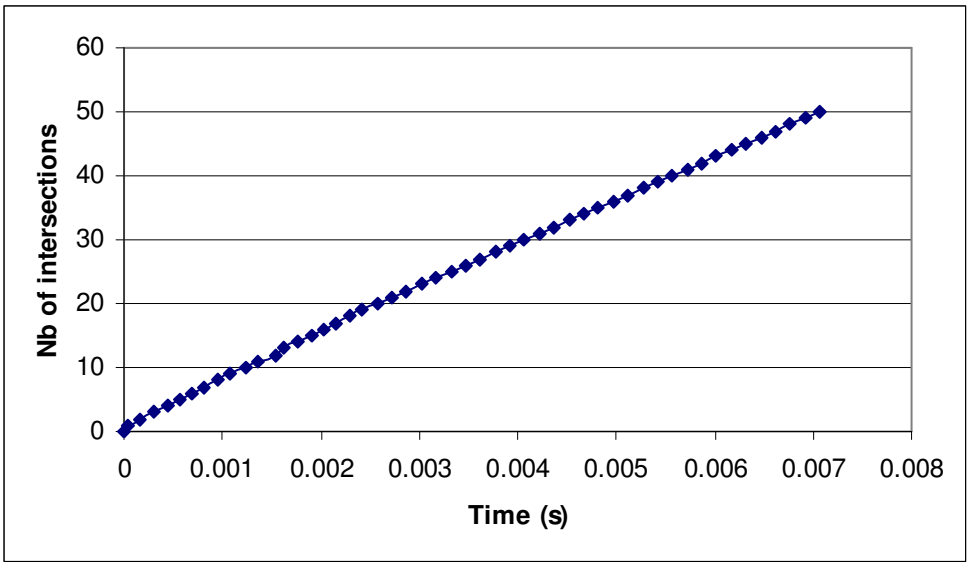

Figure 32. Number of Intersections of Figure 28 and X Axis (Half-Fringes) as a Function of Time as the Laser Is Tuned, for a Sawtooth Frequency of 5 Hz, Corresponding to a Tuning Rate of 294.6 nm/s

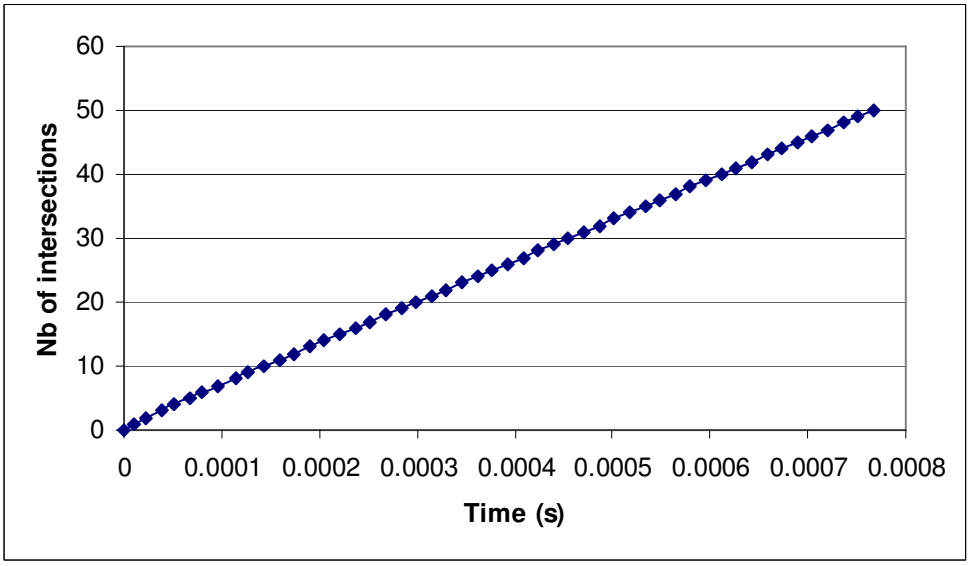

Figure 33. Number of Intersections of Figure 29 and X Axis (Half-Fringes) as a Function of Time as the Laser Is Tuned, for a Sawtooth Frequency of 50 Hz, Corresponding to a Tuning Rate of 2749.5 nm/s

The four plots indicate that the laser frequency is close to a linear function of time, thus indicating that the laser is being tuned linearly.

D. Tunable Laser Characteristics (EO Filter)

In this experiment illustrated in Figure 34, the ring cavity now includes the electro-optic tunable filter presented in Chapter III. Otherwise, the setup is the same as that illustrated in Figure 16 with the fiber FP as the tuning element.

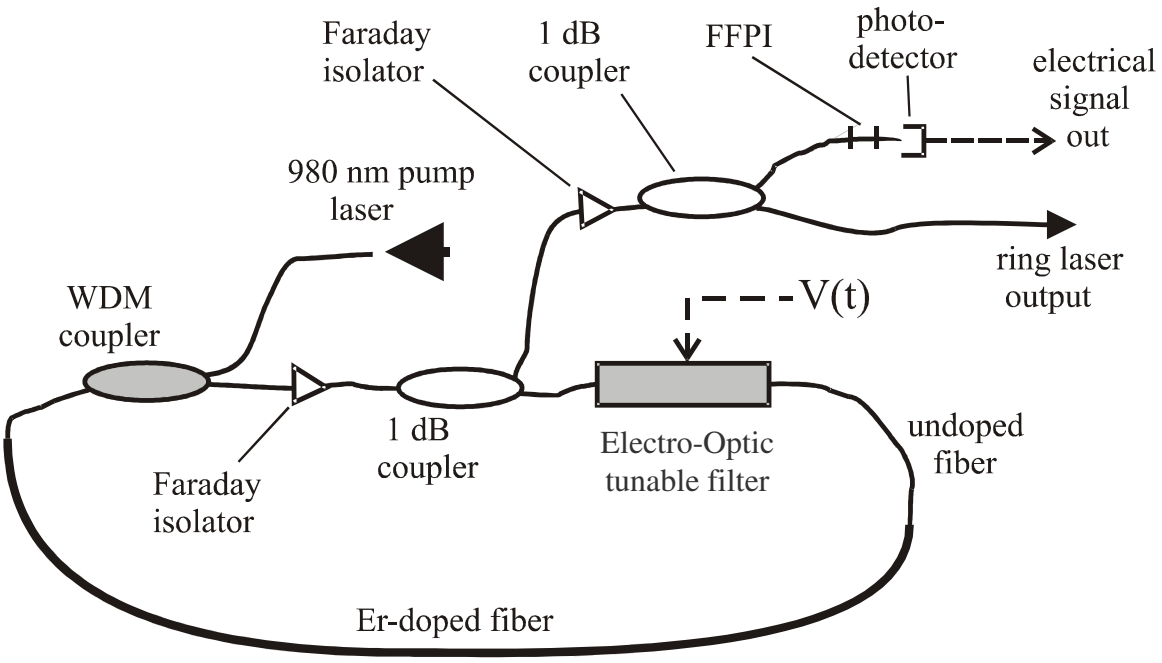

Figure 34. Tunable Ring Laser with an Electro-Optic Filter

To set up the EO filter in the laser cavity, high-precision xyz translation stages are used for aligning the input and output fibers with the filter. Three such stages, like the one depicted in Figure 35 have been purchased from Line Tool Company.

In order to obtain the best alignment between the fibers and the filter, the "ring laser output" end of Figure 34 is connected to an optical power meter. The input fiber is aligned by using an infrared card to make sure the light is going through the filter waveguide. Then, the output fiber is adjusted by moving both the coarse and fine feed attachments of the translation stage (Fig. 35) while the optical power is being monitored with the power meter. The position of the output fiber is adjusted to yield a maximum in laser output power, indicative of the best achievable alignment between the filter and the fibers.

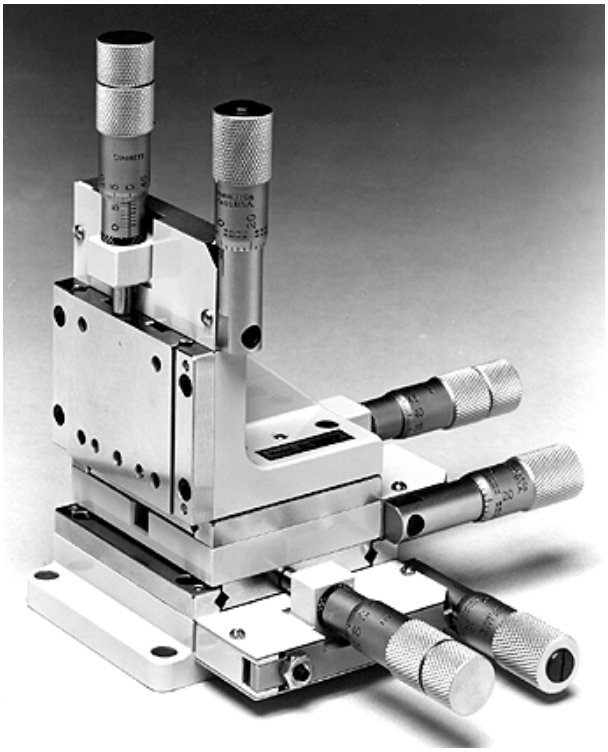

Figure 35. High-Precision Translation Stage [11]

The “ring laser output” fiber in Figure 34 is connected to the OSA. The pump current is set at 100 mA, corresponding to 47 mW of pump power. The DC voltage on the electrodes is 20 V. The results, shown in Figure 36, indicate a center wavelength of 1531.02 nm and a spectral width of 2.155 nm; they agree closely with expected values. The nearest sidelobes to the main peak are about 15 dB below the central lobe.

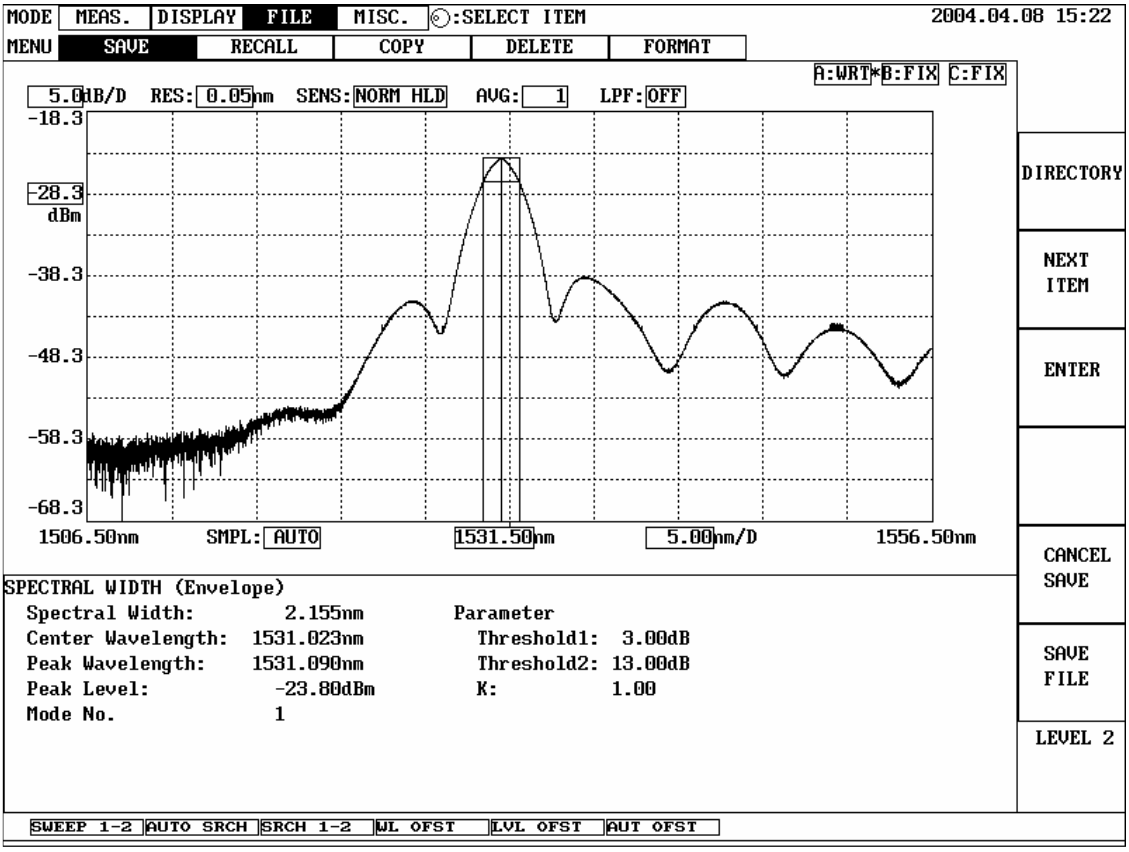

Figure 36. Laser Spectral Profile at DC Voltage = 20 V

The EO tunable filter is connected to a DC power supply and the voltage is varied manually from -60 V to 100 V. Tests have been carried out at different voltages, and data has been collected at -12 V, -5 V, 35 V, 45 V, and 50 V. The results are shown respectively in Figures 37 through 41. At -60 V, the lasing wavelength turned out to be 1526.3 nm, and then as the voltage increased, the wavelength reached 1536.9 nm.

A tuning range of about 11 nm has been achieved. The spectral width is averaged to be 2.33 nm over the entire spectrum. The peak power of every lasing profile, as observed in Figures 37 through 41, is almost fixed and the average value is measured to be around -26.6 dBm.

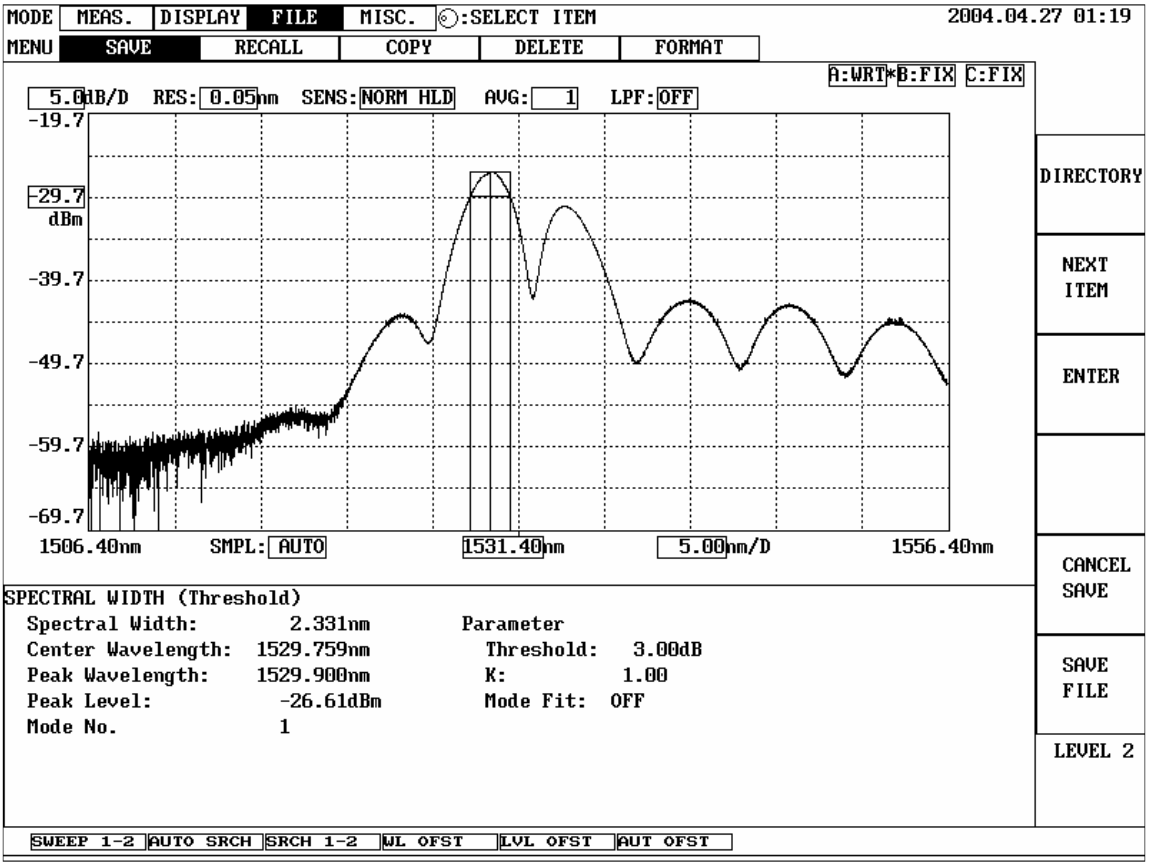

Figure 37. Laser Spectral Profile at DC Voltage = -12 V

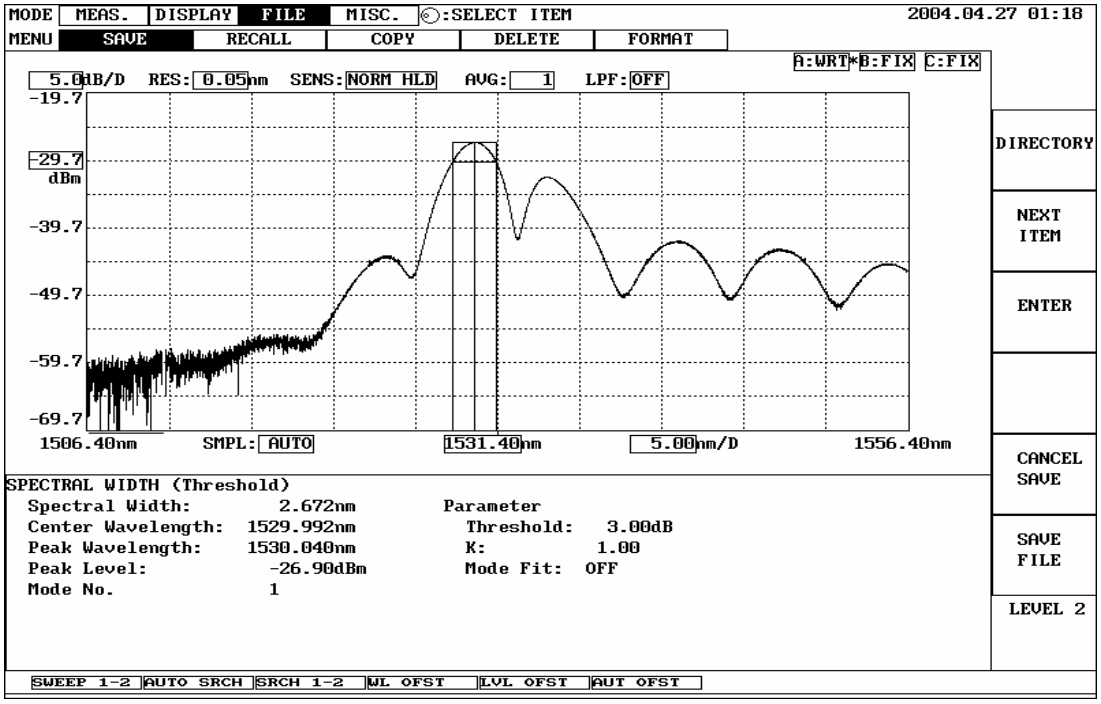

Figure 38. Laser Spectral Profile at DC Voltage = -5 V

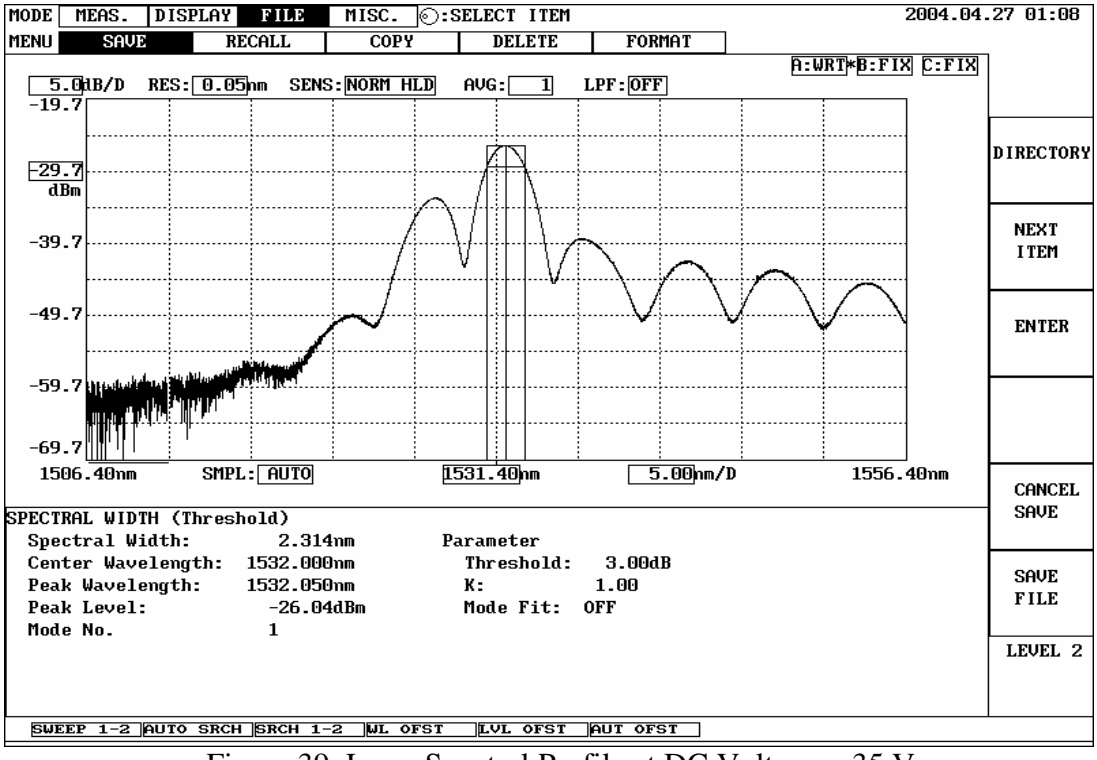

Figure 39. Laser Spectral Profile at DC Voltage = 35 V

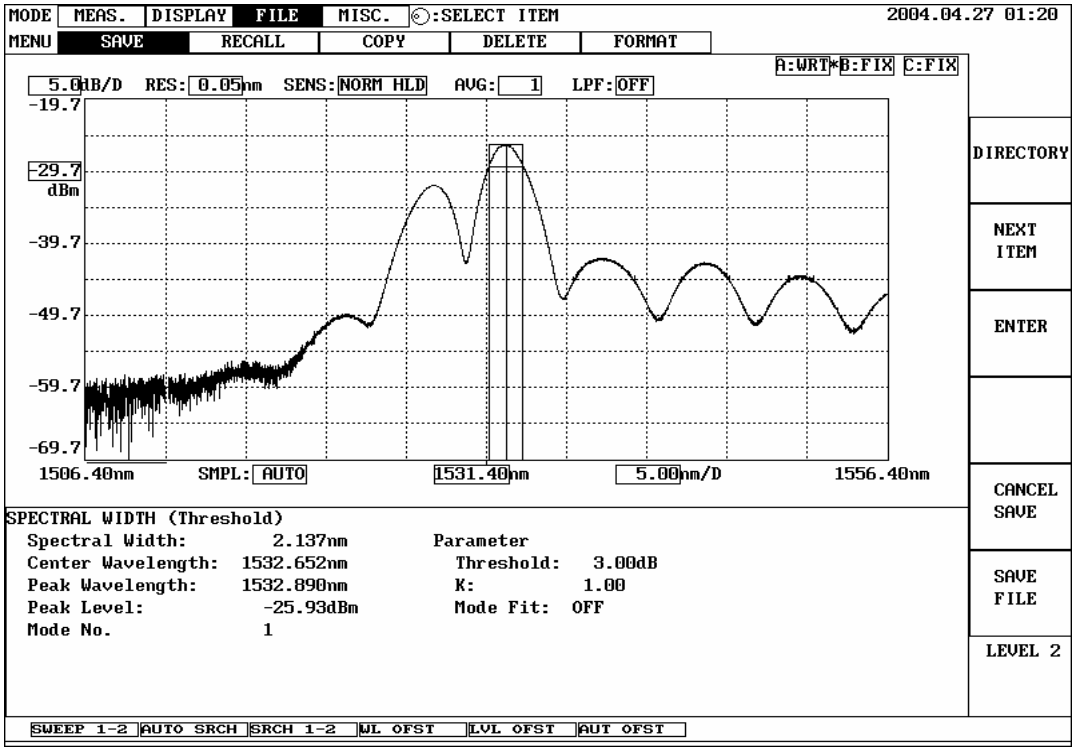

Figure 40. Laser Spectral Profile at DC Voltage = 45 V

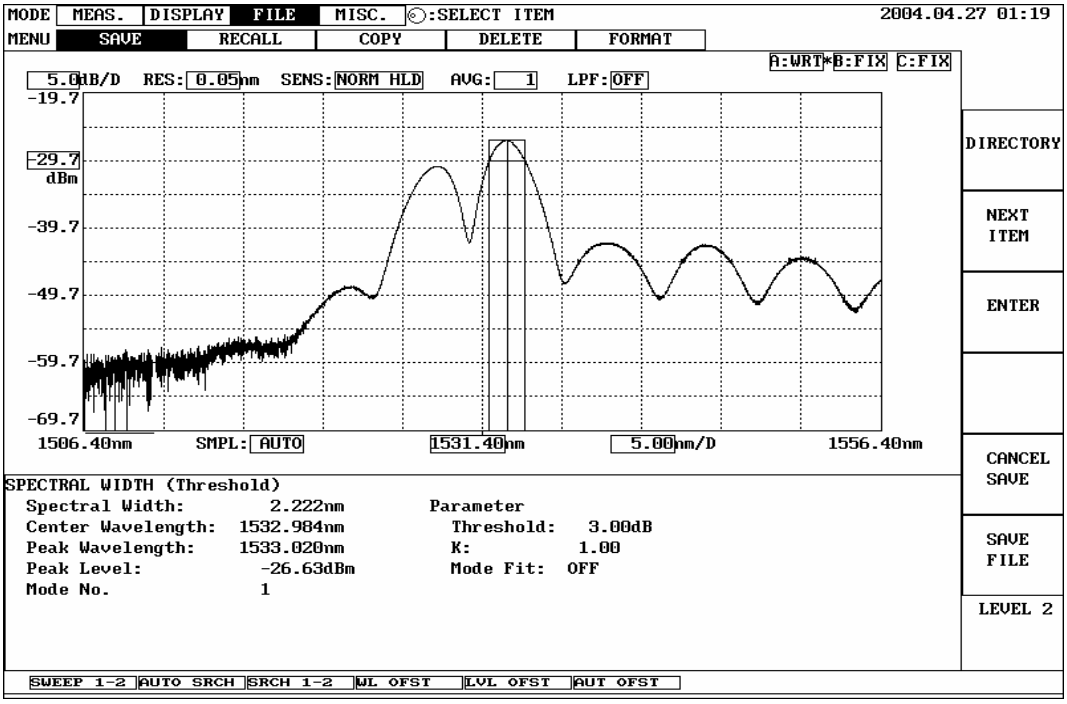

Figure 41. Laser Spectral Profile at DC Voltage = 50 V

To demonstrate the tuning linearity of the laser with the EO filter as the tuning element, the dependence of the lasing wavelength on the tuning voltage is given in Figure 42, which shows that the wavelength is close to a linear function of voltage.

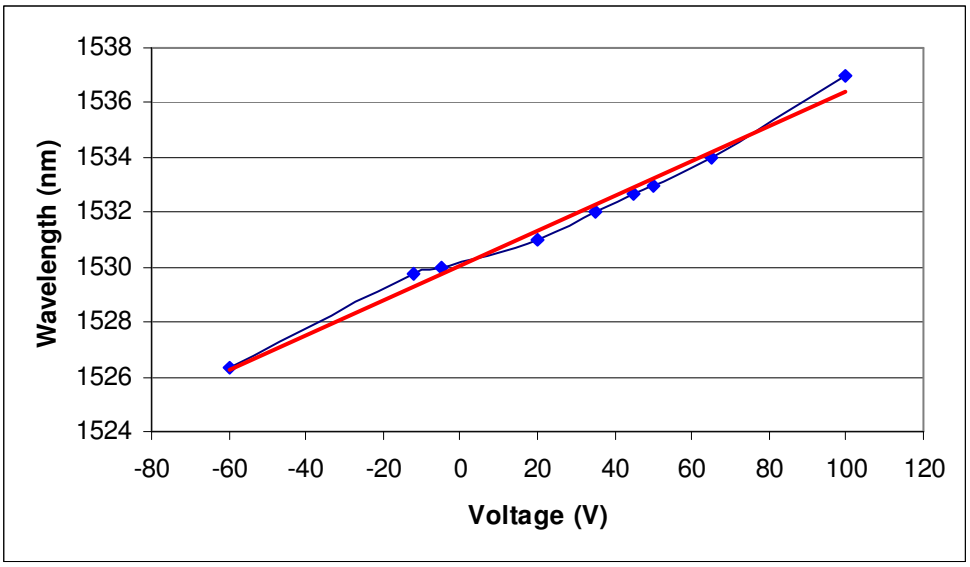

Figure 42. Wavelength vs Tuning Voltage (EO Filter)

CHAPTER V

CONCLUSIONS AND RECOMMENDATIONS

Linear tuning of the frequency of an erbium-doped fiber ring laser has been experimentally demonstrated. Both a fiber Fabry-Perot filter and an electro-optic tunable filter have been utilized as intra-cavity tuning elements. In each case, the tuning has been accomplished by driving the tuning element with a sawtooth voltage waveform, and the dynamic characteristics of the tuned laser have been studied by observing the fringes generated as the laser light is transmitted through a fiber Fabry-Perot interferometer.

In addition to a tunable filter, the laser assembly includes a pump laser, a WDM coupler, Faraday isolators, 1 dB fiber couplers and erbium-doped fiber. The laser threshold and slope efficiency were measured to be 11 mW and 11% respectively. .

Using the FP filter as the intra-cavity tuning element, the laser has been tuned over a 50 nm spectral range, from 1539 nm to 1589 nm. The spectral width of the laser output is observed to be 0.049 nm. The dynamic tuning characteristics of the laser have been investigated, and a linear tuning with time (“linear chirp”) has been achieved over the entire spectral range. When driving the FP filter with a 200 Hz sawtooth waveform, a tuning speed of 16480 nm/s was achieved. With the EO filter as the tuning element, the laser has been tuned over an 11 nm spectral range, from 1526 nm to 1537 nm. The dependence of the lasing wavelength on the tuning voltage has been investigated, and a tuning rate of 0.06 nm / V has been achieved.

An important improvement of this research would be to test the new samples of the EO filter, being fabricated at Texas A&M laboratories. These new samples would give more stability to the light signal, allowing better investigation of the tuning speeds, and the tuning range may be increased. Also, tuning speeds might be maximized by using a shorter section of the erbium-doped fiber, making the light signal travel a smaller distance in the laser cavity.

REFERENCES

[1] M.C. Amann and J. Buus, *Tunable Laser Diodes*. Norwood, MA: Artech House, 1998.

[2] P. Rigby, "Tunable lasers revisited," Jan 2003; Available: http://www.lightreading.com/document.asp?doc_id=26332.

[3] X. Wan, "The monitoring and multiplexing of fiber optic sensors using chirped laser sources," Ph.D. dissertation, Texas A&M University, College Station, 2003.

[4] X. Wan and H. F. Taylor, "Linearly chirped erbium-doped fiber laser," *IEEE Photon. Technol. Lett*., vol. 15, pp. 188-190, 2003.

[5] H. Kobrinski and K. Cheung, "Wavelength-tunable optical filters: Applications and technologies," *IEEE Communications Magazine*, pp. 53-63, Oct. 1989.

[6] H.J.R. Dutton, *Understanding Optical Communications*. Upper Saddle River, N.J.: Prentice Hall PTR, 1998.

[7] J.C. Palais, *Fiber Optic Communications*. Upper Saddle River, NJ: Prentice Hall, 1998.

[8] Micron Optics, "Fiber Fabry Perot Technology Overview," Available: http://www.micronoptics.com/telecom_ffp.htm, March 05, 2004.

[9] Y. Ping, "Two-port polarization independent electro-optically tunable wavelength filter in lithium niobate," M.S. Thesis, Texas A&M University, College Station, 2003.

[10] Y. Ping, O. Eknoyan and H.F. Taylor, "Polarization independent tunable bandpass filter in Ti:$LiNbO_3$ utilizing symmetric branch beam splitters," in *Proceedings of the Optical Communications Conference (OFC'04)*, Los Angeles, CA, Feb. 22-27, 2004.

[11] Line Tool Company, "Fine feed attachments for xyz stages," Available: http://www.linetool.net/olc/38626008/options.htm, April 02, 2004.

APPENDIX A

Fiber Fabry-Perot Tunable Filter Characteristics

OPTICAL	
Operating Wavelength Range	
S-Band	1480 to 1520 nm
C-Band	1520 to 1570 nm
L-Band	1570 to 1620 nm
C+L Band	1520 to 1620 nm
Free Spectral Range	80 pm to 250 nm (10 to 31250 GHz)
3dB Bandwidth	0.3 pm to 25 nm (40 MHz to 3125 GHz)
Standard Finesse Values	10, 40, 100, 150, 200, 650, 1000, 1500, 2000, 4000, 6000
Insertion Loss	< 2.5 dB
Polarization Dependent Loss	< 0.25 dB
Input Power	< 100 mW (for F<200)
ELECTRICAL	
Tuning Voltage / FSR	< 12 V
Capacitance	< 3.0 μF
Slew Rate	< 10 V/ms
Maximum Tuning Voltage	70 V
ENVIRONMENTAL	
Operating Temperature	-20 to 80 ^{0}C
ΔVoltage / Operating Temperature	< 12 V
ΔInsertion Loss / Operating Temperature	< 0.5 dB
ΔInsertion Loss / Vibration	< 0.5 dB
MECHANICAL	
Dimensions	12.7 x 14.3 x 57.2 mm
Weight	28 g
Mounting Holes	(4) #1-72 UNF x 0.16 inch deep
Pigtail Jacket	900 μm buffer tubing
Pigtail Length	> 1 m

VITA

Mr. Hicham Joseph Fadel was born in Naccache, Lebanon on January 07, 1980. He received the degree of Bachelor of Engineering in computer and communications engineering at the American University of Beirut in July of 2002.

Immediately after graduation, he continued his studies in the Department of Electrical Engineering at Texas A&M University by beginning his master's degree work under the direction of Dr. Henry F. Taylor. He worked as a Research Assistant from September 2003 to August 2004. His main interests of study are laser technology and optical communications.

Mailing Address: 214 Zachry Engineering Center
3128 TAMU
College Station, TX 77843-3128

The typist for this thesis was Hicham Joseph Fadel